Lattice-induced wave-function effects on trapped superfluids

Yeyang Zhang *

International Center for Quantum Materials, School of Physics, Peking University, Beijing 100871, China

(Received 25 January 2024; revised 2 August 2024; accepted 26 August 2024; published 10 September 2024)

Wave-function effects in uncorrelated systems are characterized by the Berry curvature and quantum metric. Beyond those, we propose gauge-independent tensors describing Bloch wave-function effects on local interaction between correlated particles. We derive an effective hydrodynamic theory for ultracold bosons in optical lattices. Ground states and collective modes of superfluids in isotropic harmonic traps are solved for highly symmetric lattices. In a dynamic process, the wave-function effects are featured by the eigenfrequency, amplitude, and phase shift of an excited breathing mode and can be observed in experiments. We also give a tight-binding model of a bipartite square lattice with nontrivial wave-function effects, where results are estimated with typical experimental parameters. Our discovery advances the connections between the modern band theory and quantum many-body physics.

DOI: 10.1103/PhysRevA.110.033310

I. INTRODUCTION

Quantum systems are traditionally featured by the eigenenergies of Hamiltonians. Lattices modify the low-energy spectra of electrons or atoms through effective mass [1,2]. Eigenstates of quantum systems are also crucial for physical observables. As global properties of Bloch wave functions, topological indices distinguish insulator phases [3–8] and lead to quantized Hall conductances [9–18]. Local properties of wave functions are quantified by the quantum geometric tensor, i.e., the Berry curvature and quantum metric [19–21]. Quantum geometric effects on linear [22–26] and nonlinear [27–32] transport have been widely studied.

Wave-function effects of single-particle Bloch states play important roles even in many-body systems. It indicates possible fractional Chern insulators [33–35] and stabilizes superfluid [36–39] or superconductor [40–50] phases in flat-band systems. For trapped interacting bosonic atoms in optical lattices [51–55], the wave-function effects on hydrodynamic equations have been proposed based on the Berry curvature [56,57]. However, the spatial density fluctuation of atoms is comparable with the lattice for a ground state, so it is improper to treat the interaction as a slowly varying mean-field potential as in the literature. Matrix elements between two-body Bloch states are necessary to characterize the correlation between particles. Despite some results of Bogoliubov excitation spectra [58,59], a hydrodynamic theory extracting the wave-function effects beyond the single-body quantum geometric tensor is still lacking.

In this paper, we derive a low-energy effective hydrodynamic theory of locally interacting bosons in an optical lattice with an additional external potential. The spatial variation of the external potential is assumed to be small compared with the lattice, so a generalized effective mass theory with a gradient expansion [60] applies to the system. Distinct from the single-body external potential, in the second order of momentum, a ϕ^4 interaction is corrected by one scalar, one vector, and three second-order symmetric tensors. Those quantities characterize *lattice-induced (Bloch) wave-function effects* of the system. All of the quantities are invariant under a gauge transformation in the momentum space. One of the second-order tensors is related to inverse participation ratios [61] of Bloch wave functions in a unit cell. Another is odd under time reversal, whose symmetry is forbidden in the quantum geometric tensor. For a three-dimensional (3D) lattice of the cubic crystal system or a two-dimensional (2D) lattice with a $\mathbb{Z}_n$ ($n \geqslant 3$) rotational symmetry, the effective theory becomes isotropic when the external potential is central. Without time-reversal symmetry, the Thomas-Fermi distribution [57,62] for a ground state is corrected with a finite spatial variation of the phase of bosons.

Our corrections to the hydrodynamic theory stem from a different physical origin, compared with those due to quantum fluctuations, e.g., the Lee-Huang-Yang correction [63,64]. Although both of them are many-body effects, the lattice-induced wave-function effects are already displayed in the classical limit of the boson field. In a weakly interacting limit in 2D or 3D, where the interaction becomes small enough while chemical potential keeps in the same order, the quantum fluctuation corrections are negligible compared with the lattice corrections. The classical hydrodynamic description is valid in this limit. The results in this paper are derived therein and can be generalized with the quantum fluctuations.

For measurable predictions, we solve collective modes in a harmonic trap [65–68] for the isotropic cases. The ground state depends on the lattice potential, so the collective modes can be excited and observed by suddenly varying the optical lattice at some time. In the leading order of the gradient expansion, values of the scalar and two of the three second-order tensors describing the lattice-induced wave-function effects can be differentiated experimentally. When the wave-function

*Contact author: yeyzhang@pku.edu.cn

effects are weak, they are directly linked to three observables, the frequency, amplitude, and initial phase of a breathing mode. To make a nonzero initial phase, the time-reversal symmetry needs to be broken. As a concrete example of tight-binding models, we consider a bilayer square lattice in a nonuniform synthetic magnetic field [69–71], whose Bloch wave-function effects are only exhibited with interaction. Therein, the main results of this paper are estimated with typical orders of magnitude of experimental parameters [72–77]. Although the lattice model is a theoretical prototype, essential physics is shown, and our framework applies to general superfluids in lattices.

This paper is structured as follows. In Sec. II, we derive the continuous-space effective theory of superfluids in lattices with ϕ^4 interaction and show the lattice-induced effective corrections to the interaction. In Sec. III, we calculate the hydrodynamic properties of the superfluids based on the effective theory, including ground states and collective modes of the system. We also discuss when the quantum fluctuations are negligible compared with the lattice-induced corrections. In Sec. IV, we apply the hydrodynamic theory where the external potential is the isotropic harmonic trap. In particular, we propose the direct observables of the lattice-induced wave-function effects. In Sec. V, we provide the tight-binding example with nontrivial wave-function effects. A brief summary and outlook are given in Sec. VI. Technical details for deriving the effective interaction and solving the collective modes in the harmonic trap are shown in Appendix A and Appendix B, respectively. Further discussions on tight-binding modes are offered in Appendix C.

II. EFFECTIVE THEORY OF SUPERFLUIDS IN LATTICES

We start from a continuous model of bosonic atoms in d dimensions. The Hamiltonian of the system is given by three parts, $H = H_0 + H_U + H_I$. Here, H_0 is a single-body Hamiltonian with an optical lattice and is diagonalized in a Bloch basis ($\hbar = 1$),

$$H_0 = \sum_{\mathsf{n}} \int_{\mathrm{BZ}} d^d\boldsymbol{k} b^\dagger_{\mathsf{n},\boldsymbol{k}} \epsilon_{\mathsf{n}}(\boldsymbol{k}) b_{\mathsf{n},\boldsymbol{k}}, \tag{1}$$

where n is a band index and BZ denotes an integral in the first Brillouin zone. The bottom of the lowest band ($\mathsf{n} = 0$) is assumed at $\boldsymbol{k} = \boldsymbol{0}$, around which there is a quadratic dispersion, $\epsilon_0(\boldsymbol{k}) \approx \frac{k^2}{2m}$. Bosonic operators in the real space and Bloch space are linked by Bloch wave functions,

$$a(\boldsymbol{r}) = \sum_{\mathsf{n}} \int_{\mathrm{BZ}} d^d\boldsymbol{k} e^{i\boldsymbol{k}\cdot\boldsymbol{r}} u_{\mathsf{n},\boldsymbol{k}}(\boldsymbol{r}) b_{\mathsf{n},\boldsymbol{k}}. \tag{2}$$

$u_{\mathsf{n},\boldsymbol{k}}(\boldsymbol{r})$ is normalized such that the average of $|u_{0,\boldsymbol{k}}(\boldsymbol{r})|^2$ in a unit cell equals $(2\pi)^{-d}$. H_U is an applied external potential and H_I is a local repulsive interaction between atoms,

$$\begin{aligned} H_U &= \int_\infty d^d\boldsymbol{r} a^\dagger(\boldsymbol{r}) U(\boldsymbol{r}) a(\boldsymbol{r}), \\ H_I &= \frac{g}{2} \int_\infty d^d\boldsymbol{r} a^\dagger(\boldsymbol{r}) a^\dagger(\boldsymbol{r}) a(\boldsymbol{r}) a(\boldsymbol{r}). \end{aligned} \tag{3}$$

In cold-atom systems, it is proper to model the interaction to be short ranged [62,78,79], even at the length scale of the optical lattice. The spatial variation of $U(\boldsymbol{r})$ is assumed to be small compared with the lattice, such that the Fourier components of $U(\boldsymbol{r})$ outside the first Brillouin zone are negligible [60]. In addition, supposing only the excitation of Bloch states near the band bottom of the lowest band are considered in a low-energy effective theory, the position index $\boldsymbol{r}$ of a Wannier basis $b_{\mathsf{n}}(\boldsymbol{r})$ (i.e., a Fourier transform of the Bloch basis) is approximated to be continuous in an effective theory. Those assumptions require that the typical energy and momentum scales of the external potential are much smaller than those of the chemical potential and band dispersion. Those assumptions apply to ground states and low-energy hydrodynamic collective modes with slowly varying $U(\boldsymbol{r})$ (see Secs. III and IV).

Taking hydrodynamic variables, i.e., $b(\boldsymbol{r}) = \sqrt{n(\boldsymbol{r})} e^{i\theta(\boldsymbol{r})}$, and letting the field variables depend on time, we get an effective action in the (coarse-grained) Wannier basis by a second-order expansion of the (quasi)momentum $\boldsymbol{k}$,

$$\mathcal{S} = \int dt \left[\int_\infty d^d\boldsymbol{r}(-n\partial_t\theta + \mu n) - H_0 - H_U - H_I \right], \tag{4}$$

where the theory has been projected to the lowest band (the band index is omitted) and μ is a chemical potential. The free Hamiltonian of quasiparticles reads

$$H_0 = \int_\infty d^d\boldsymbol{r} \frac{1}{2m} \left[\frac{(\nabla n)^2}{4n} + n(\nabla\theta)^2 \right]. \tag{5}$$

A. Effective external potential

The effective correction to the external potential by the Berry curvature (Ω_γ) and quantum metric ($\mathsf{g}_{\alpha\beta}$) have been derived in the literature [60],

$$\begin{aligned} H_U = \int_\infty d^d\boldsymbol{r} \Big[& Un + \frac{1}{2}\mathsf{g}_{\alpha\beta}(\boldsymbol{0}) n \partial_\alpha\partial_\beta U \\ & - \frac{1}{2}\boldsymbol{\Omega}(\boldsymbol{0}) \cdot (\nabla U \times \nabla\theta) n \Big], \end{aligned} \tag{6}$$

$$\begin{aligned} \Omega_\gamma(\boldsymbol{k}) &= \frac{1}{2}\epsilon_{\alpha\beta\gamma}\Omega_{\alpha\beta} = \frac{1}{2}\epsilon_{\alpha\beta\gamma}\big[\partial_{k_\alpha} A_\beta(\boldsymbol{k}) - \partial_{k_\beta} A_\alpha(\boldsymbol{k})\big], \\ \mathsf{g}_{\alpha\beta}(\boldsymbol{k}) &= \frac{1}{2}\big[\langle\partial_{k_\alpha} u_{\boldsymbol{k}}|(1 - |u_{\boldsymbol{k}}\rangle\langle u_{\boldsymbol{k}}|)|\partial_{k_\beta} u_{\boldsymbol{k}}\rangle + (\alpha \leftrightarrow \beta)\big], \\ A_\alpha(\boldsymbol{k}) &= i\langle u_{\boldsymbol{k}}|\partial_{k_\alpha} u_{\boldsymbol{k}}\rangle. \end{aligned} \tag{7}$$

A gauge transformation $u_{\boldsymbol{k}} \to u_{\boldsymbol{k}} e^{i\vartheta_{\boldsymbol{k}}}$ has been applied when deriving Eq. (6) such that the result becomes "gauge independent,"

$$\vartheta_{\boldsymbol{k}} = A_\alpha(\boldsymbol{0})k_\alpha + \tfrac{1}{4}\big[\partial_{k_\alpha} A_\beta(\boldsymbol{0}) + \partial_{k_\beta} A_\alpha(\boldsymbol{0})\big] k_\alpha k_\beta. \tag{8}$$

Actually, the result is gauge dependent, while it equals a gauge-independent quantity in the specific gauge.

Note that $n(\boldsymbol{r})$ in Eq. (4) also depends on the gauge. As an observable, the (gauge-independent) physical density of the atoms, $n_{\mathrm{ph}}(\boldsymbol{r})$, should be derived from the physical external potential $U(\boldsymbol{r})$,

$$n_{\mathrm{ph}}(\boldsymbol{r}) = -\frac{\delta\mathcal{S}}{\delta U(\boldsymbol{r})} = n + (\nabla n)\cdot(\nabla\theta \times \boldsymbol{\Omega}) + \frac{1}{2}\mathsf{g}_{\alpha\beta}\partial_\alpha\partial_\beta n. \tag{9}$$

Here the time argument is omitted and $U(\boldsymbol{r},t)=U(\boldsymbol{r})$. The physical density can also be obtained when counting the chemical potential μ into the external potential $U(\boldsymbol{r})$. Because μ is a constant, from Eq. (6) we know the result given by Eq. (9) is unaffected by such substitution.

B. Effective interaction

To derive an effective interaction, we write the ϕ^4 interaction in the Bloch basis,

$$\frac{2}{g}H_I=\frac{1}{(2\pi)^d}\int_{\mathrm{BZ}}\left(\prod_{i=1}^{3}d^d\boldsymbol{k}_i\right)b^\dagger_{\boldsymbol{k}_1}b^\dagger_{\boldsymbol{k}_2}b_{\boldsymbol{k}_3}b_{\boldsymbol{k}_4}\langle\!\langle u_{\boldsymbol{k}_1}u_{\boldsymbol{k}_2}|u_{\boldsymbol{k}_3}u_{\boldsymbol{k}_4}\rangle\!\rangle, \tag{10}$$

where $\boldsymbol{k}_4\equiv\boldsymbol{k}_1+\boldsymbol{k}_2-\boldsymbol{k}_3$,

$$\langle\!\langle u_{\boldsymbol{k}_1}u_{\boldsymbol{k}_2}|u_{\boldsymbol{k}_3}u_{\boldsymbol{k}_4}\rangle\!\rangle\equiv\frac{(2\pi)^{2d}}{\Omega_{\mathrm{cell}}}\int_{\mathrm{cell}}d^d\boldsymbol{r}u^*_{\boldsymbol{k}_1}(\boldsymbol{r})u^*_{\boldsymbol{k}_2}(\boldsymbol{r})u_{\boldsymbol{k}_3}(\boldsymbol{r})u_{\boldsymbol{k}_4}(\boldsymbol{r}), \tag{11}$$

"cell" denotes an integral in the unit cell, and Ω_{cell} is the volume of the unit cell. A relation has been applied when taking a sum over lattice vectors $\boldsymbol{R}$,

$$\sum_{\boldsymbol{R}}e^{i(\boldsymbol{k}_3+\boldsymbol{k}_4-\boldsymbol{k}_1-\boldsymbol{k}_2)\cdot\boldsymbol{R}}=\frac{(2\pi)^d}{\Omega_{\mathrm{cell}}}\delta^d(\boldsymbol{k}_1+\boldsymbol{k}_2-\boldsymbol{k}_3-\boldsymbol{k}_4). \tag{12}$$

Only half of the first Brillouin zone near the band bottom has been considered such that reciprocal scattering has been neglected. We further approximate the integral domain of momenta in Eq. (10) to be infinity to get an effective theory in the continuous space.

Then we can apply a second-order expansion of momentum. We get a zeroth-order term [51],

$$H_{I0}=\frac{g}{2}\int_\infty d^d\boldsymbol{r}M(\boldsymbol{0})n(\boldsymbol{r})^2, \tag{13}$$

a first-order term,

$$H_{I1}=\frac{g}{2}\int_\infty d^d\boldsymbol{r}M'_\alpha(\boldsymbol{0})n^2(\partial_\alpha\theta), \tag{14}$$

and a second-order term (see Appendix A 1),

$$H_{I2}=\frac{g}{2}\int_\infty d^d\boldsymbol{r}\Big[\frac{1}{2}M''_{\alpha\beta}(\boldsymbol{0})n^2(\partial_\alpha\theta)(\partial_\beta\theta) - 2\tilde{S}_{\alpha\beta}(\boldsymbol{0})n(\partial_\alpha n)(\partial_\beta\theta)+W_{\alpha\beta}(\boldsymbol{0})(\partial_\alpha n)(\partial_\beta n)\Big], \tag{15}$$

where

$$M(\boldsymbol{k})=\langle\langle u_{\boldsymbol{k}}u_{\boldsymbol{k}}|u_{\boldsymbol{k}}u_{\boldsymbol{k}}\rangle\rangle =1+\frac{(2\pi)^{2d}}{\Omega_{\mathrm{cell}}}\int_{\mathrm{cell}}d^d\boldsymbol{r}\Big[|u_{\boldsymbol{k}}(\boldsymbol{r})|^2-\frac{1}{(2\pi)^d}\Big]^2\geqslant 1, \tag{16}$$

$$M'_\alpha(\boldsymbol{k})=\partial_{k_\alpha}M(\boldsymbol{k}),\ M''_{\alpha\beta}(\boldsymbol{k})=\partial_{k_\alpha}\partial_{k_\beta}M(\boldsymbol{k}),$$
$$W_{\alpha\beta}(\boldsymbol{k})=\tfrac{3}{8}M''_{\alpha\beta}(\boldsymbol{k})-P_{\alpha\beta}(\boldsymbol{k}) =\tfrac{3}{8}M''_{\alpha\beta}(\boldsymbol{k})-\langle\!\langle\partial_{k_\alpha}(u^*_{\boldsymbol{k}}u_{\boldsymbol{k}})|\partial_{k_\beta}(u^*_{\boldsymbol{k}}u_{\boldsymbol{k}})\rangle\!\rangle,$$
$$\widetilde{S}_{\alpha\beta}(\boldsymbol{k})=\mathrm{Im}\big[\langle\!\langle u_{\boldsymbol{k}}u_{\boldsymbol{k}}|u_{\boldsymbol{k}}\partial_{k_\alpha}\partial_{k_\beta}u_{\boldsymbol{k}}\rangle\!\rangle - \langle\!\langle u_{\boldsymbol{k}}u_{\boldsymbol{k}}|\big(\partial_{k_\alpha}u_{\boldsymbol{k}}\big)\big(\partial_{k_\beta}u_{\boldsymbol{k}}\big)\rangle\!\rangle\big]. \tag{17}$$

TABLE I. The permutation and time-reversal symmetries of the gauge-independent second-order tensors characterizing the lattice-induced wave-function effects. "+" and "−" denote even and odd parities, respectively. The parities of $S_{\alpha\beta}$ are different from either $\mathsf{g}_{\alpha\beta}$ or $\Omega_{\alpha\beta}$.

	$\mathsf{g}_{\alpha\beta}$	$\Omega_{\alpha\beta}$	$M''_{\alpha\beta}$	$W_{\alpha\beta}$	$S_{\alpha\beta}$
Permutation	+	−	+	+	+
Time reversal	+	−	+	+	−

By choosing the same gauge in Eq. (8) as in Eq. (6), an effective interaction $H_I=H_{I0}+H_{I1}+H_{I2}$ is also gauge independent (see Appendix A 2). $M(\boldsymbol{k})$ itself is "gauge independent," while $\widetilde{S}_{\alpha\beta}(\boldsymbol{0})$ equals a gauge-independent quantity $S_{\alpha\beta}(\boldsymbol{0})$ in this gauge,

$$S_{\alpha\beta}(\boldsymbol{k})=\mathrm{Im}\big[\langle\!\langle u_{\boldsymbol{k}}u_{\boldsymbol{k}}|u_{\boldsymbol{k}}\partial_{k_\alpha}\partial_{k_\beta}u_{\boldsymbol{k}}\rangle\!\rangle-\langle\!\langle u_{\boldsymbol{k}}u_{\boldsymbol{k}}|\big(\partial_{k_\alpha}u_{\boldsymbol{k}}\big)\big(\partial_{k_\beta}u_{\boldsymbol{k}}\big)\rangle\!\rangle - M(\boldsymbol{k})\langle u_{\boldsymbol{k}}|\partial_{k_\alpha}\partial_{k_\beta}u_{\boldsymbol{k}}\rangle\big]. \tag{18}$$

The argument $\boldsymbol{k}$ of the *Bloch wave-function quantities*, Ω_γ, $\mathsf{g}_{\alpha\beta}$, M, M'_α, $M''_{\alpha\beta}$, $W_{\alpha\beta}$, and $S_{\alpha\beta}$, will be omitted when $\boldsymbol{k}=\boldsymbol{0}$.

Note that the "double Dirac notation" defined in Eq. (11) is not an inner product between two-body states. Instead, it is a matrix element of the interaction between two-body states. For the ϕ^4 interaction, the matrix element $M(\boldsymbol{k})$ takes the (quartic) inverse participation ratio of the Bloch wave function in the unit cell, quantifying the gathering of particles. We can see that the lattice-induced corrections to the interaction are qualitatively distinct from those to the external potential (see Table I). Contrary to $\Omega_{\alpha\beta}$, the three tensors $M''_{\alpha\beta}$, $W_{\alpha\beta}$, and $S_{\alpha\beta}$ appearing in the effective interaction are all symmetric tensors. In addition, while $S_{\alpha\beta}$ is symmetric, it is odd under time reversal. So the quantum geometric tensor $\mathcal{B}_{\alpha\beta}=\mathsf{g}_{\alpha\beta}+i\Omega_{\alpha\beta}$ is not sufficient to describe lattice-induced wave-function effects in the correlated system.

III. HYDRODYNAMIC THEORY

In a hydrodynamic theory neglecting quantum corrections, classical equations of motion of a superfluid are determined by $\delta\mathcal{S}=\delta\int dtd^d\boldsymbol{r}\mathcal{L}(n,\theta)=0$,

$$\begin{aligned}\partial_t\theta=&-\frac{1}{2m}(\boldsymbol{\nabla}\theta)^2+\frac{\nabla^2 n}{4mn}+\frac{(\boldsymbol{\nabla}n)^2}{8mn^2}\\&-\Big(U+\frac{1}{2}\mathsf{g}_{\alpha\beta}\partial_\alpha\partial_\beta U\Big)-\frac{1}{2}\boldsymbol{\nabla}\theta\cdot(\boldsymbol{\nabla}U\times\boldsymbol{\Omega})\\&+\mu-gMn-gM'_\alpha n\partial_\alpha\theta-\frac{g}{2}M''_{\alpha\beta}n(\partial_\alpha\theta)(\partial_\beta\theta)\\&-gS_{\alpha\beta}n\partial_\alpha\partial_\beta\theta+gW_{\alpha\beta}\partial_\alpha\partial_\beta n,\end{aligned} \tag{19}$$

$$\begin{aligned}\partial_t n=&-\boldsymbol{\nabla}\cdot\Big(\frac{n}{m}\boldsymbol{\nabla}\theta+\frac{n}{2}\boldsymbol{\nabla}U\times\boldsymbol{\Omega}\Big)\\&-\partial_\alpha\Big(\frac{g}{2}M'_\alpha n^2+\frac{g}{2}M''_{\alpha\beta}n^2\partial_\beta\theta-gS_{\alpha\beta}n\partial_\beta n\Big).\end{aligned} \tag{20}$$

The chemical potential μ is included on the right-hand side of Eq. (19). Thereby, we absorb an unobservable uniform phase winding $\partial_t\theta=-\mu$ for ground states without external

potential [62]. Equation (20) is a continuity equation,

$$\partial_t n + \nabla \cdot (n\boldsymbol{v}) = 0, \tag{21}$$

where

$$v_\alpha = \frac{1}{m}\partial_\alpha\theta + \frac{1}{2}\epsilon_{\alpha\beta\gamma}(\partial_\beta U)\Omega_\gamma + \frac{g}{2}M'_\alpha n + \frac{g}{2}M''_{\alpha\beta}n\partial_\beta\theta - gS_{\alpha\beta}\partial_\beta n. \tag{22}$$

A. Ground state and collective modes without external potential

We first simply discuss the ground state of the system when $U(\boldsymbol{r}) = 0$. Suppose ∇n and $\nabla\theta$ are small. Then, at the leading order, Eq. (19) gives $n(\boldsymbol{r}) = n_0 = \frac{\mu}{gM}$. However, $\theta(\boldsymbol{r})$ is determined by

$$\left(\frac{1}{m}\delta_{\alpha\beta} + \frac{gn_0}{2}M''_{\alpha\beta}\right)\partial_\beta\theta = -\frac{gn_0}{2}M'_\alpha. \tag{23}$$

When M'_α is small but finite, $\theta(\boldsymbol{r})$ acquires a finite momentum. For a general M'_α, we cannot apply the expansion of $\nabla\theta$. In the remainder of the paper, we only consider the case of $M'_\alpha = 0$. It can be realized when there is an inversion symmetry, when there is a $\mathbb{Z}_n$ ($n \geqslant 3$) rotational symmetry for 2D, or when a 3D lattice belongs to the cubic crystal system. In this case, there is a uniform ground state,

$$n(\boldsymbol{r}) = n_0 = \frac{\mu}{gM}, \quad \theta(\boldsymbol{r}) = \theta_0. \tag{24}$$

The system has a typical energy scale μ and a typical momentum scale $\sqrt{m\mu}$, and they can form other typical scales with different dimensions. In the remainder of the paper, for ground states and low-energy collective modes with $U(\boldsymbol{r})$, we further assume that reduced by the two typical scales, $\nabla^n U$ and $\nabla^n\theta$ (including $\partial_t^n\theta$) are nth-order small quantities (which can be verified *a posteriori*), and the Bloch wave-function quantities are, at most, $O(1)$. Note that $\nabla(n - n_0)$ and $\nabla\theta$ do not need to be in the same order [see Eqs. (25) and (31)]. The results of the remainder of the paper will be derived in the leading order of this gradient expansion. A correction of the density in Eq. (9) is second order, so we take $n_{\rm ph}(\boldsymbol{r}, t) = n(\boldsymbol{r}, t)$.

With $n = n_0 + \delta n$, we get the leading order of the equations of motion,

$$\partial_t^2\theta = -gM\partial_t\delta n = \frac{gMn_0}{m}\nabla^2\theta + \frac{g^2Mn_0^2}{2}M''_{\alpha\beta}\partial_\alpha\partial_\beta\theta. \tag{25}$$

The $d \times d$ real symmetric matrix $M''_{\alpha\beta}$ has d eigenvalues $\lambda_1, \ldots, \lambda_d$, so the system is anisotropic in general and we get d sound velocities [58,59],

$$c_i = \sqrt{\frac{gMn_0}{m} + \frac{g^2Mn_0^2}{2}\lambda_i} = \sqrt{\frac{\mu}{m} + \frac{\lambda_i\mu^2}{2M}} \quad (i = 1, \ldots, d). \tag{26}$$

B. Ground state with external potential

When $U(\boldsymbol{r}) \neq 0$, a static solution of the system is determined by $\partial_t\theta = \partial_t n = 0$. Suppose the ground state of $U(\boldsymbol{r}) \neq 0$ is static and adiabatically connected to the ground state of $U(\boldsymbol{r}) = 0$. Denote the ground state as $b(\boldsymbol{r}) = \sqrt{n_0(\boldsymbol{r})}e^{i\theta_0(\boldsymbol{r})}$. From Eq. (19), in the leading order, we get

$$n_0(\boldsymbol{r}) = \begin{cases} \frac{\mu - U(\boldsymbol{r})}{gM} & \text{when} \quad \mu > U(\boldsymbol{r}) \\ 0 & \text{when} \quad \mu \leqslant U(\boldsymbol{r}). \end{cases} \tag{27}$$

When $n(\boldsymbol{r})$ is fixed, the Lagrangian $\mathcal{L}$ becomes a quadratic form of $\nabla\theta$. To minimize the quadratic form, we cannot simply require $\boldsymbol{v}(n_0, \theta_0) = \boldsymbol{0}$ because $n\boldsymbol{v}$ is not rotation free in general. In the leading order, to solve $\theta_0(\boldsymbol{r})$, we can take n in Eq. (20) to be n_0. As ∇U is proportional to ∇n_0, the antisymmetric term of the Berry curvature vanishes. Then, $\theta_0(\boldsymbol{r})$ is determined by

$$\left[\frac{n_0}{m}\delta_{\alpha\beta} + \frac{g}{2}M''_{\alpha\beta}n_0^2\right]\partial_\alpha\partial_\beta\theta_0 + \left[\frac{1}{m}\delta_{\alpha\beta} + gM''_{\alpha\beta}n_0\right](\partial_\alpha n_0)(\partial_\beta\theta_0) = \frac{1}{2}gS_{\alpha\beta}\partial_\alpha\partial_\beta n_0^2. \tag{28}$$

When the time-reversal symmetry is broken such that $S_{\alpha\beta} \neq 0$, it is nontrivial to determine $\theta_0(\boldsymbol{r})$. In the remainder of the paper, we focus on a simple case where the external potential is central, i.e., $U(\boldsymbol{r}) = U(r)$. Furthermore, suppose the lattice belongs to the cubic crystal system in 3D or there is a $\mathbb{Z}_n$ ($n \geqslant 3$) rotational symmetry in 2D. For those highly symmetric cases, $M'_\alpha = 0$, $\mathsf{g}_{\alpha\beta} = \mathsf{g}\delta_{\alpha,\beta}$, $M''_{\alpha\beta} = M''\delta_{\alpha,\beta}$, $W_{\alpha\beta} = W\delta_{\alpha,\beta}$, $S_{\alpha\beta} = S\delta_{\alpha,\beta}$; $\boldsymbol{\Omega} = \Omega\hat{\boldsymbol{e}}_z$ for 2D and $\boldsymbol{\Omega} = \boldsymbol{0}$ for 3D. The stability of the ground state without $U(r)$ requires

$$\eta \equiv \frac{M''m\mu}{M} > -2. \tag{29}$$

Suppose the ground-state configuration is isotropic. Then we get the rotation-free part of the velocity for $n(\boldsymbol{r}) = n(r)$, $\theta(\boldsymbol{r}) = \theta(r)$,

$$\tilde{\boldsymbol{v}} \equiv \boldsymbol{v} - \frac{1}{2}(\nabla U) \times \boldsymbol{\Omega} = \left(\frac{1}{m} + \frac{gM''}{2}n\right)\nabla\theta - gS\nabla n. \tag{30}$$

The ground state is given by $\tilde{\boldsymbol{v}}(n_0, \theta_0) = \boldsymbol{0}$, as a term $n\nabla\theta \cdot (\nabla U \times \boldsymbol{\Omega})$ in the Lagrangian $\mathcal{L}$ vanishes. For $\mu > U(r)$, we get

$$\left[\frac{1}{m} + \frac{M''}{2M}(\mu - U)\right]\nabla\theta_0 = -\frac{S}{M}\nabla U. \tag{31}$$

According to Eqs. (27) and (31), small ∇U justifies the momentum expansion of ∇n_0 and $\nabla\theta_0$.

Equation (27) is the same as the Thomas-Fermi distribution [57,62] (except a constant factor M). However, Eq. (31) gives a correction to the Thomas-Fermi distribution, which cannot be obtained when the interaction between atoms is treated as a mean field [56,57]. $\nabla\theta_0$ becomes nonzero and in the same order as ∇U. Although an equilibrium distribution of $\theta_0(\boldsymbol{r})$ may not be observed directly, there are observable effects when the equilibrium distribution depends on time due to the manipulation of the optical lattice. An observable dynamic process thereby will be discussed in Sec. IV B 2.

C. Collective modes with external potential

Consider collective modes near the isotropic static ground state, $n(\boldsymbol{r},t)=n_0(r)+\delta n(\boldsymbol{r},t)$, $\theta(\boldsymbol{r},t)=\theta_0(r)+\delta\theta(\boldsymbol{r},t)$. We take the double expansion of derivatives of U and $\delta\theta$ in Eqs. (19) and (20), and calculate leading-order equations of motion. Similar to the case of $U(r)=0$, δn is in the same order as $\partial_t\delta\theta$,

$$\partial_t\delta\theta=-gM\delta n, \tag{32}$$

where we have used the condition that $\partial_t\delta\theta=0$ when $\delta\theta=\delta n=0$. For $\mu>U(r)$, Eq. (21) gives

$$\begin{aligned}\partial_t^2\delta n&=-\nabla\cdot(n_0\partial_t\boldsymbol{v})-\nabla\cdot(\delta n\partial_t\boldsymbol{v})\\&\quad-\nabla\cdot\left[(\partial_t\delta n)\tfrac{1}{2}(\nabla U)\times\boldsymbol{\Omega}\right]-\nabla\cdot[(\partial_t\delta n)\tilde{\boldsymbol{v}}]\\&\approx-\nabla\cdot(n_0\partial_t\boldsymbol{v}).\end{aligned} \tag{33}$$

Here the first term on the right-hand side is in the same order as $\partial_t^2\delta n$, which will be verified in Eq. (34). The second term is neglected because δn makes it one order higher than $\partial_t^2\delta n$. The third term is neglect because ∇U makes it one order higher than $\partial_t^2\delta n$, although a correction of the Berry curvature was discussed in previous works [56,57]. The last term is neglected because $\tilde{\boldsymbol{v}}(n_0,\theta_0)=0$, so terms in $\tilde{\boldsymbol{v}}$ are proportional to $\nabla\delta\theta$ or δn, which makes the last term one order higher than $\partial_t^2\delta n$. Then, for $\mu>U(r)$, $\delta n(\boldsymbol{r},t)$ is given by

$$\begin{aligned}\partial_t^2\delta n&\approx-\nabla\cdot\left[\frac{\mu-U}{gM}\left(\frac{1}{m}\nabla\partial_t\delta\theta+\frac{g}{2}M''\frac{\mu-U}{gM}\nabla\partial_t\delta\theta\right)\right]\\&=\nabla\cdot(\mu-U)\left[\frac{1}{m}\nabla\delta n+\frac{M''}{2M}(\mu-U)\nabla\delta n\right]\\&=\frac{\mu-U}{m}\left[1+\frac{\eta}{2}\left(1-\frac{U}{\mu}\right)\right]\nabla^2\delta n\\&\quad-\frac{\nabla U}{m}\cdot\left[1+\eta\left(1-\frac{U}{\mu}\right)\right]\nabla\delta n.\end{aligned} \tag{34}$$

Here we also neglected the terms proportional to $\nabla\partial_t\delta n$ and $(\partial_t\delta n)\nabla\delta\theta$ in $\partial_t\boldsymbol{v}$ because their orders are one higher than $\nabla\partial_t\delta\theta$. Compared with Eqs. (26) and (27), we know that the first term in Eq. (34) is to replace the constant density n_0 by the density distribution $n_0(\boldsymbol{r})$. The two terms in Eq. (34) are both important when the momentum scales of U and δn are in the same order.

D. Discussion on quantum fluctuations

In this section, we derive the lattice-induced corrections to the hydrodynamic theory in the classical-field limit, i.e., $\delta\mathcal{S}=0$. In addition, quantum fluctuations may also give corrections. Typically, the quantum-fluctuation corrections are small (e.g., about 1%) [63,64]. However, it should be clarified in what limit our treatment is justified. The ratio between the quantum correction to the particle density $n_{\rm q}$ and classical density $n_{\rm cl}$ vanishes in a weakly interacting limit ($d=2,3$),

$$\frac{n_{\rm q}}{n_{\rm cl}}\sim\frac{\xi_h^{-d}}{\mu/g}\sim\frac{(m\mu)^{\frac{d}{2}}}{\mu/g}=m^{\frac{d}{2}}\mu^{\frac{d}{2}-1}g\to0, \tag{35}$$

where the particle density $n=n_{\rm cl}+n_{\rm q}$, and ξ_h is the typical length scale (i.e., healing length [62]) of the superfluid state. Equation (35) guarantees the applicability of the hydrodynamic theory. On the other hand, the lattice-induced corrections may survive in this limit. Suppose the interaction strength g decreases while the particle density n increases, such that the chemical potential μ keeps in the same order. Then, from the classical equations of motion given by Eqs. (19) and (20), or from the results given by Eqs. (26), (27), (31), and (34), we can see that the lattice-induced corrections remain in the same order, despite the suppression of the quantum corrections. Therefore, it is fair to stay on this limit and neglect the quantum fluctuations in this paper. Our derivations can be generalized when further taking the quantum fluctuations into consideration.

IV. SUPERFLUID DYNAMICS IN A HARMONIC TRAP

In cold-atom systems, $U(r)$ is commonly taken as an isotropic harmonic potential [62],

$$U(r)=\frac{1}{2}m\omega_0^2r^2\equiv\mu\frac{r^2}{R^2}. \tag{36}$$

Here, $\omega_0\ll\mu\lesssim J$ and $k_0\equiv\frac{1}{R}\ll\sqrt{m\mu}\lesssim k_M$ such that the gradient expansion (i.e., momentum and frequency expansion) is applicable for $r<R$. J is the bandwidth of the lowest band and k_M is the momentum range of the first Brillouin zone.

A. Collective modes

Define $\rho(\frac{\boldsymbol{r}}{R},t)\equiv\delta n(\boldsymbol{r},t)$. The solutions of Eqs. (34) and (36) depend on η. For the 3D case with spherical coordinates $\boldsymbol{r}=(r,\theta,\phi)$,

$$\rho(\boldsymbol{r},t)=\sum_{\mathsf{n},\ell,\mathsf{m}}\sum_{\xi=\pm}e^{-i\xi\omega_{\mathsf{n},\ell}t}\mathsf{a}_{\mathsf{n},\ell,\mathsf{m},\xi}\rho_{\mathsf{n},\ell}(r)Y_{\ell,\mathsf{m}}(\theta,\phi), \tag{37}$$

where $Y_{\ell,\mathsf{m}}$ are spherical harmonics. Then we get a one-dimensional eigenequation for $\rho_{\mathsf{n},\ell}(r)$ with $0<r<1$,

$$\begin{aligned}-\omega_{\mathsf{n},\ell}^2\rho_{\mathsf{n},\ell}&=\frac{1}{2}\omega_0^2(1-r^2)\left[1+\frac{\eta}{2}(1-r^2)\right]\left[\frac{d^2}{dr^2}+\frac{2}{r}\frac{d}{dr}\right.\\&\quad\left.-\frac{\ell(\ell+1)}{r^2}\right]\rho_{\mathsf{n},\ell}-\omega_0^2r[1+\eta(1-r^2)]\frac{d}{dr}\rho_{\mathsf{n},\ell}.\end{aligned} \tag{38}$$

For the 2D case with polar coordinates $\boldsymbol{r}=(r,\phi)$,

$$\rho(\boldsymbol{r},t)=\sum_{\mathsf{n},\mathsf{m}}\sum_{\xi=\pm}e^{-i\xi\omega_{\mathsf{n},|\mathsf{m}|}t}\mathsf{a}_{\mathsf{n},\mathsf{m},\xi}\rho_{\mathsf{n},|\mathsf{m}|}(r)e^{i\mathsf{m}\phi}. \tag{39}$$

Then we get

$$\begin{aligned}-\omega_{\mathsf{n},|\mathsf{m}|}^2\rho_{\mathsf{n},|\mathsf{m}|}&=\frac{1}{2}\omega_0^2(1-r^2)\left[1+\frac{\eta}{2}(1-r^2)\right]\left[\frac{d^2}{dr^2}+\frac{1}{r}\frac{d}{dr}\right.\\&\quad\left.-\frac{\mathsf{m}^2}{r^2}\right]\rho_{\mathsf{n},|\mathsf{m}|}-\omega_0^2r[1+\eta(1-r^2)]\frac{d}{dr}\rho_{\mathsf{n},|\mathsf{m}|}.\end{aligned} \tag{40}$$

In Eqs. (37) and (39), n takes non-negative integers.

When $\eta\neq0$, eigenfrequencies (eigenenergies) $\omega_{\mathsf{n},\mathsf{j}}$ cannot be obtained analytically, where $\mathsf{j}\equiv\ell$ for $d=3$ and $\mathsf{j}\equiv|\mathsf{m}|$ for

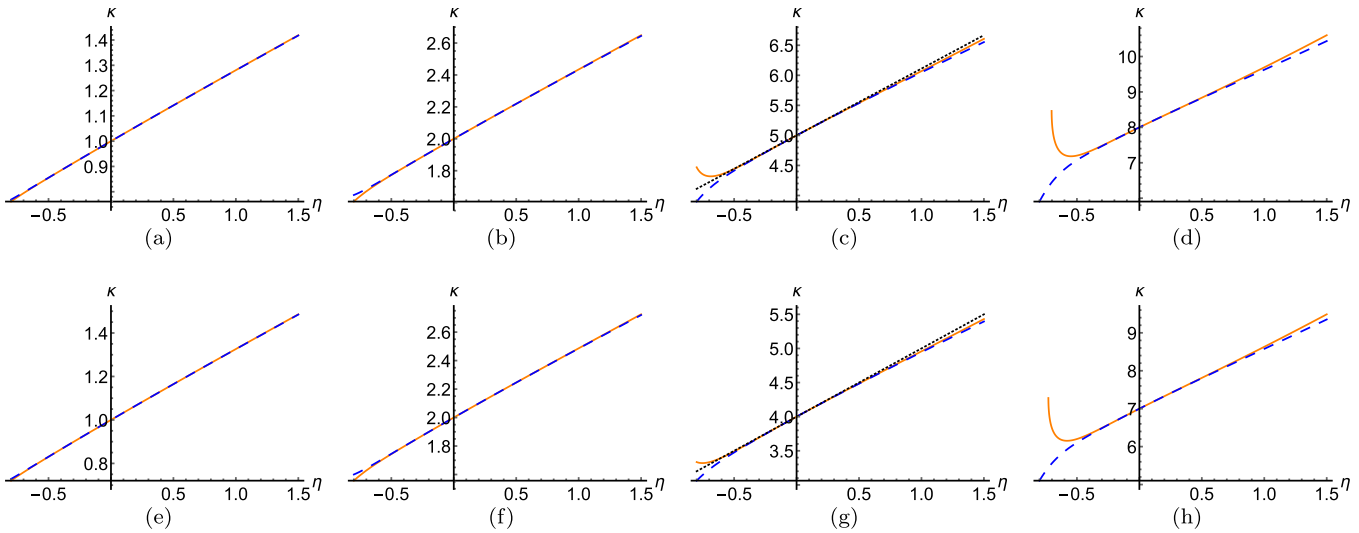

FIG. 1. Numerical results of eigenfrequencies of collective modes ($\omega_{\mathsf{n},\mathsf{j}} \equiv \omega_0\sqrt{\kappa}$) in an isotropic harmonic trap as functions of the quantity $\eta = \frac{M''m\mu}{M}$. Here, κ and η are dimensionless. (a)–(d) for 3D ($\mathsf{j} = \ell$); (e)–(h) for 2D ($\mathsf{j} = |\mathsf{m}|$). Parameters are taken to be (a),(e) $(\mathsf{n}, \mathsf{j}) = (0, 1)$, (b),(f) $(\mathsf{n}, \mathsf{j}) = (0, 2)$, (c),(g) $(\mathsf{n}, \mathsf{j}) = (1, 0)$, and (d),(h) $(\mathsf{n}, \mathsf{j}) = (1, 1)$. Orange solid curves are for $\mathsf{k}_0 = 4$ and blue dashed curves are for $\mathsf{k}_0 = 5$ defined in Eq. (42). The results are convergent where the differences between the solid and dashed curves are much smaller than the averages. The two curves almost coincide for most of the data of $\eta > -1$, and thus it shows good numerical convergence. When n or $|\eta|$ increases, larger k_0 is needed for convergence. In addition, we plot black dotted lines in (c) and (g) according to the first-order perturbation theory [see Eq. (49) with $\eta \approx m\mu M''$], where κ is linear in η. The perturbative results are consistent with the numerical results.

$d = 2$. Nevertheless, when $\eta > -1$, solutions take the form of an infinite series,

$$\rho_{\mathsf{n},\mathsf{j}}(r) = \sum_{\mathsf{k}=0}^{\infty} \alpha_{\mathsf{n},\mathsf{j},2\mathsf{k}} r^{2\mathsf{k}+\mathsf{j}}, \tag{41}$$

and the eigenfrequencies are solvable numerically [80]. According to an asymptotic analysis of $\alpha_{\mathsf{n},\mathsf{j},2\mathsf{k}}$ (see Appendix B 2), we can iteratively determine $\frac{\alpha_{\mathsf{n},\mathsf{j},2\mathsf{k}+2}}{\alpha_{\mathsf{n},\mathsf{j},2\mathsf{k}}}$ as functions of $\omega_{\mathsf{n},\mathsf{j}}$ for $\mathsf{k} \leqslant \mathsf{k}_0$, and obtain $\omega_{\mathsf{n},\mathsf{j}}$ (see Fig. 1) by requiring

$$\frac{\alpha_{\mathsf{n},\mathsf{j},2\mathsf{k}_0+2}}{\alpha_{\mathsf{n},\mathsf{j},2\mathsf{k}_0}} = \frac{\mathsf{k}_0}{\mathsf{k}_0+1}\frac{\eta}{\eta+2}, \tag{42}$$

with a certain integer k_0 large enough for convergence. For several low-energy levels, i.e., n and j are not large, the eigenfrequency $\omega_{\mathsf{n},\mathsf{j}}$ is in the same order as ω_0. According to Eqs. (32) and (34) with $\omega_0 \ll \mu$, this justifies the momentum and frequency expansion of δn_0 and $\delta\theta_0$ for the low-energy collective modes. When $\eta = 0$, Eq. (42) returns to the condition that the series becomes finite [65] and the numerical results in Fig. 1 are consistent with those without the lattice.

In addition, collective modes are normalizable and satisfy an orthonormal relation [81] (see Appendix B 3 for a proof),

$$\int_0^1 r^{d-1}\rho^*_{\mathsf{n}_1,\mathsf{j}}(r)\rho_{\mathsf{n}_2,\mathsf{j}}(r)dr = \delta_{\mathsf{n}_1,\mathsf{n}_2}. \tag{43}$$

The orthonormal condition is independent of η, which enables perturbative solutions of the collective modes in Sec. IV B 1.

B. Breathing mode with weak lattice-induced wave-function effects

From Eqs. (27), (29), and (31) and Fig. 1, in the leading order of the gradient expansion, we know $M_d \equiv M - 1$, M'', and S are already involved in the dynamics of the superfluid in the isotropic harmonic trap [82]. To demonstrate more explicit relations between the three Bloch wave-function quantities and experimental observables, suppose the lattice-induced wave-function effects are weak,

$$M_d \equiv M - 1 \ll 1, \quad m\mu|M''| \ll 1, \quad m\mu|S| \ll 1. \tag{44}$$

The last condition in Eq. (44) can be weakened and substituted by $m\omega_0|S| \ll 1$, which has been automatically satisfied by previously imposed conditions $m\mu|S| = O(1)$ and $\omega_0 \ll \mu$. We will keep the leading order of the three quantities, which leads to $|\eta| \approx |M''|m\mu \ll 1$.

The weak wave-function effects can be realized by a weak lattice potential. They can also be effectively realized in a tight-binding limit by weakly breaking sublattice symmetry, where the integrals of $\boldsymbol{r}$ in the definition Eq. (11) should be renormalized and become summations of a sublattice index (see Appendix C 1). Here we define the sublattice symmetry physically, i.e., by permuting the sublattices, which may be different from a conventional one [3–6].

As an example, we focus on the lattice-induced wave-function effects on the breathing mode ($\mathsf{n} = 1$, $\mathsf{j} = 0$) [62]. As explained below Eq. (42), the momentum and frequency expansion is valid for the breathing mode. Without the wave-function effects, (zeroth-order) eigenvalues ($\kappa_{\mathsf{n},\mathsf{j}} \equiv \frac{\omega^2_{\mathsf{n},\mathsf{j}}}{\omega_0^2}$) and

normalized eigenfunctions ($\rho_{\mathsf{n},\mathsf{j}}$) of Eqs. (38) and (40) for the breathing mode are given by (see Appendix B 1 and Ref. [65])

$$\kappa_{1,0}^{(0)} = \begin{cases} 5 & \text{for } 3\text{D} \\ 4 & \text{for } 2\text{D}, \end{cases} \tag{45}$$

$$\rho_{1,0}^{(0)} = \begin{cases} \frac{3\sqrt{7}}{2}\left(1-\frac{5}{3}r^2\right) & \text{for } 3\text{D} \\ \sqrt{6}(1-2r^2) & \text{for } 2\text{D}. \end{cases} \tag{46}$$

1. Eigenfrequency

At the first order, $\kappa_{1,0}$ should be a linear function of η, i.e., a linear function of M''. We can apply a perturbation theory similar to that in quantum mechanics and get the first-order correction to the eigenvalue $\kappa_{1,0}$,

$$\kappa_{1,0}^{(1)} = \int_0^1 r^{d-1}\rho_1^{(0)}\hat{L}^{(1)}\rho_1^{(0)}dr = \begin{cases} \frac{10}{9}\eta & \text{for } 3\text{D} \\ \eta & \text{for } 2\text{D}, \end{cases} \tag{47}$$

where the first-order operator $\hat{L}^{(1)}$ with $\ell = 0$ is given by

$$\hat{L}^{(1)} = \begin{cases} -\frac{\eta}{4}(1-r^2)^2\frac{d^2}{dr^2} & \\ -\frac{\eta}{2}(1-r^2)(1-3r^2)\frac{1}{r}\frac{d}{dr} & \text{for } 3\text{D} \\ -\frac{\eta}{4}(1-r^2)^2\frac{d^2}{dr^2} & \\ -\frac{\eta}{4}(1-r^2)(1-5r^2)\frac{1}{r}\frac{d}{dr} & \text{for } 2\text{D}. \end{cases} \tag{48}$$

So the first-order eigenfrequency of the breathing mode reads

$$\omega_{1,0} = \begin{cases} \sqrt{5}\omega_0\left(1+\frac{1}{9}m\mu M''\right) & \text{for } 3\text{D} \\ 2\omega_0\left(1+\frac{1}{8}m\mu M''\right) & \text{for } 2\text{D}. \end{cases} \tag{49}$$

2. Amplitude and initial phase in a dynamic process

To further show the effects of M_d and S, we consider a dynamic process. Atoms are initially at the ground state with the harmonic potential, satisfying the Thomas-Fermi distribution. There is no lattice or a tight-binding lattice with negligible Bloch wave-function effects, i.e., $M_d = M'' = S = 0$. At time $t = 0$, we suddenly open or change the lattice potential to make the weak lattice-induced wave-function effects. Then the ground-state distribution is substituted by Eqs. (27) and (31), and the atoms are at an excited state.

Suppose, for $t < 0$, the chemical potential, the effective mass of atoms, the typical frequency of the harmonic traps, and the trapping radius of the atoms are $\tilde{\mu}, \tilde{m}, \tilde{\omega}, \tilde{R}$. For $t > 0$, they become μ, m, ω, R. Because $U(r)$ does not change, we have

$$\tfrac{1}{2}m\omega_0^2 r^2 = \tfrac{1}{2}\tilde{m}\tilde{\omega}_0^2 r^2, \tag{50}$$

$$\mu = \tfrac{1}{2}m\omega_0^2 R^2, \quad \tilde{\mu} = \tfrac{1}{2}\tilde{m}\tilde{\omega}_0^2\tilde{R}^2. \tag{51}$$

In addition, suppose the amount of atoms remains invariant during the process,

$$\frac{\mu}{gM}\int_0^R\left(1-\frac{r^2}{R^2}\right)r^{d-1}dr = \frac{\tilde{\mu}}{g}\int_0^{\tilde{R}}\left(1-\frac{r^2}{\tilde{R}^2}\right)r^{d-1}dr. \tag{52}$$

Combining Eqs. (50)–(52) with Eqs. (27) and (31), we get initial conditions at $t = 0$,

$$\rho(\boldsymbol{r},0) \approx \begin{cases} \frac{\mu}{g}M_d\left(\frac{3}{5}-r^2\right) & \text{for } 3\text{D} \\ \frac{\mu}{g}M_d\left(\frac{1}{2}-r^2\right) & \text{for } 2\text{D}, \end{cases} \tag{53}$$

$$\frac{d}{dr}\delta\theta(\boldsymbol{r},0) \approx 2m\mu S\frac{r}{R^2}, \tag{54}$$

$$\partial_t\delta n(\boldsymbol{r},0) \approx -\nabla\cdot(n_0\boldsymbol{v}) \approx -\nabla\cdot\left(\hat{\boldsymbol{e}}_{\boldsymbol{r}}\frac{n_0}{m}\frac{d}{dr}\delta\theta\right). \tag{55}$$

Equation (53) is not valid for $\frac{\tilde{R}}{R} < r < 1$. However, that region leads to a higher-order contribution. Equations (54) and (55) further give

$$\partial_t\rho(\boldsymbol{r},0) = \begin{cases} -\frac{m\mu}{g}\omega_0^2 S(3-5r^2) & \text{for } 3\text{D} \\ -\frac{2m\mu}{g}\omega_0^2 S(1-2r^2) & \text{for } 2\text{D}. \end{cases} \tag{56}$$

To satisfy the initial conditions given by Eqs. (53) and (56), for $t > 0$, $\rho(r,t)$ takes a form

$$\rho(\boldsymbol{r},t) = \sum_{\mathsf{n}}\mathsf{b}_{\mathsf{n},0}\rho_{\mathsf{n},0}(r)\cos(\omega_{\mathsf{n},0}t+\varphi_{\mathsf{n},0}), \tag{57}$$

where amplitudes ($\mathsf{b}_{\mathsf{n},0}$) and initial phases ($\varphi_{\mathsf{n},0}$) are determined,

$$\mathsf{b}_{\mathsf{n},0}\cos\varphi_{\mathsf{n},0} = \int_0^1 r^{d-1}\rho(r,0)\rho_{\mathsf{n},0}(r)dr, \tag{58}$$

$$\omega_{\mathsf{n},0}\mathsf{b}_{\mathsf{n},0}\sin\varphi_{\mathsf{n},0} = -\int_0^1 r^{d-1}\partial_t\rho(r,0)\rho_{\mathsf{n},0}(r)dr. \tag{59}$$

At the leading order, we can take $\rho_{\mathsf{n},0}(r) = \rho_{\mathsf{n},0}^{(0)}(r)$. Then we get the amplitude and initial phase of the breathing mode,

$$\mathsf{b}_{1,0}\cos\varphi_{1,0} = \begin{cases} \frac{2\mu M_d}{5\sqrt{7}g} & \text{for } 3\text{D} \\ \frac{\mu M_d}{2\sqrt{6}g} & \text{for } 2\text{D}, \end{cases} \tag{60}$$

$$\mathsf{b}_{1,0}\sin\varphi_{1,0} = \begin{cases} \frac{2m\mu\omega_0 S}{\sqrt{35}g} & \text{for } 3\text{D} \\ \frac{m\mu\omega_0 S}{\sqrt{6}g} & \text{for } 2\text{D}. \end{cases} \tag{61}$$

The phase shift $\varphi_{1,0}$ can be observed by a corresponding time shift, $\tau_{1,0} \equiv \frac{\varphi_{1,0}}{\omega_0}$. A nonzero phase shift $\varphi_{1,0}$ is a characteristic of time-reversal symmetry breaking.

When M_d and $m\mu S$ are in the same order, despite $|\varphi_{1,0}| \ll 1$, it is possible to observe the time shift as $\tau_{1,0} = O(\mu^{-1})$. In addition, even if $|\varphi_{1,0}| \ll 1$, when the corrections to $\omega_{1,0}$ and $\rho_{1,0}$ in the next-to-leading order are considered, a correction to $\varphi_{1,0}$ is also in the next-to-leading order.

V. TIGHT-BINDING EXAMPLE

A nonzero S can be generally realized by a synthetic magnetic field breaking the time-reversal symmetry. For a toy model showing essential physics, we consider a 2D tight-binding model of a bilayer square lattice in a nonuniform magnetic field, where the $\mathbb{Z}_4$ rotational symmetry remains intact,

$$H_0 = \sum_{i,j}(a_{i,A}^\dagger, a_{i,B}^\dagger)(\boldsymbol{h}_0)_{i,j}\begin{pmatrix} a_{j,A} \\ a_{j,B}\end{pmatrix},$$

$$\frac{(\boldsymbol{h}_0)_{i,j}}{a_L^2} = \begin{pmatrix} \Delta\delta_{i,j} - t_1\delta_{\langle i,j\rangle} & -t_2\delta_{i,j} - t_3 e^{-i\theta_3}\delta_{\langle i,j\rangle} \\ -t_2\delta_{i,j} - t_3 e^{i\theta_3}\delta_{\langle i,j\rangle} & -\Delta\delta_{i,j} - t_1\delta_{\langle i,j\rangle}\end{pmatrix}. \tag{62}$$

Here, $\boldsymbol{i}$ and $\boldsymbol{j}$ are two-dimensional site positions, A and B are two layers, and a_L is the edge length of a unit cell. $\delta_{\langle i,j\rangle} = 1$

when $\boldsymbol{i}$ and $\boldsymbol{j}$ are the nearest-neighbor sites in the 2D plane and vanishes for other cases. $t_{1,2,3}$ are positive hopping coefficients. Δ is an on-site potential breaking the sublattice symmetry of the two layers. θ_3 is a phase of the complex interlayer hopping between neighboring 2D sites. When $\sin\theta_3 \neq 0$, the complex hopping breaks both the time-reversal symmetry and sublattice symmetry. The complex hopping can be induced by an in-plane synthetic magnetic field rotating around every vertical bond.

The Hamiltonian in the momentum space reads

$$\begin{aligned}(\boldsymbol{H}_0)_{\boldsymbol{k}} = {}& \Delta\boldsymbol{\sigma}_z - 2t_1[\cos(k_x a_L) + \cos(k_y a_L)]\boldsymbol{\sigma}_0 - t_2\boldsymbol{\sigma}_x \\ & - 2t_3\cos\theta_3[\cos(k_x a_L) + \cos(k_y a_L)]\boldsymbol{\sigma}_x \\ & - 2t_3\sin\theta_3[\cos(k_x a_L) + \cos(k_y a_L)]\boldsymbol{\sigma}_y. \end{aligned} \tag{63}$$

When Δ and θ_3 are small, we get (see Appendix C 2)

$$\begin{aligned} m = \frac{1}{2(t_1+t_3)a_L^2}, \quad M_d = \frac{\Delta^2}{(t_2+4t_3)^2}, \\ M'' = \frac{8}{3}W = \frac{4a_L^2 t_3\Delta^2}{(t_2+4t_3)^3}, \quad S = -\frac{a_L^2 t_2 t_3\theta_3\Delta}{(t_2+4t_3)^3}. \end{aligned} \tag{64}$$

The Bloch wave-function quantities (M_d, M'', W, S) are proportional to Δ^2 or $\theta_3\Delta$, so they vanish when the sublattice symmetry is restored. This is reasonable because they characterize the sublattice structures of Bloch wave functions. S is proportional to θ_3 as it is time-reversal odd. Moreover, the quantum geometric tensor $\mathcal{B} = \mathsf{g} + i\Omega = 0$ at $\boldsymbol{k} = \boldsymbol{0}$ because it only contains first-order derivatives of wave functions. Although $\mathcal{B} = 0$, there are still lattice-induced wave-function effects, which are clearly beyond the traditional description.

We can estimate orders of magnitude of the Bloch wave-function quantities and resulting observables in typical experimental setups of cold atoms (e.g., Rb^{87}). Typical wavelength and strength of lasers, chemical potential of atoms, and harmonic confinement [72–77] give $a_L \sim 1$ μm, $t_{1,2,3} \sim \mu \sim 1$ kHz, $\omega_0 \sim 10$ Hz. The condition $\omega_0 \ll \mu \sim t_{1,2,3}$ is satisfied, so the gradient expansion applies to the hydrodynamic theory. To evaluate Δ and $t_3\theta_3$, we take them at a typical order of a mass breaking sublattice symmetry or time-reversal symmetry [75], $\Delta \sim t_3\theta_3 \sim 100$ Hz. Then, Eq. (64) leads to $M_d \sim m\mu M'' \sim m\mu S \sim 0.01$. According to Eqs. (49), (60), and (61), experimental observables are obtained, $\delta\omega_{1,0} \sim 0.1$ Hz, $\mathsf{b}_{1,0}/\bar{n}_0 \sim 10^{-2}$, $\tau_{1,0} \sim 1$ ms. Here, $\delta\omega_{1,0}$ is the lattice correction to $\omega_{1,0}$, $\bar{n}_0 \sim \mu/g$ is the average density of the atoms, and the relative amplitude of density, $\mathsf{b}_{1,0}/\bar{n}_0$, can be detected by the absorption strength of light [83,84]. In this example, the lattice corrections are about 1%, which is small but may be in the same order as the quantum-fluctuation corrections discussed in Sec. III D. In this case, the two kinds of corrections should be added together.

VI. SUMMARY AND OUTLOOK

In this paper, we study lattice-induced wave-function effects on correlations between bosonic particles in lattices. The hydrodynamic properties of superfluids are influenced by a richer structure of Bloch wave functions beyond the single-body quantum geometric tensor. The lattice-induced wave-function effects can be observed by the dynamic distribution of the particle density.

Our discussions are restricted to the simplest quantum many-body system where the interaction is local and the resulting effective theory is isotropic. The author wishes this paper promotes further exploration and application of wave-function effects in wider many-body systems.

In addition, the discussions are still based on single-body Bloch wave functions. We derive the results at a practical level. Namely, this paper aims to propose specific many-body physical effects of Bloch wave functions, instead of clarifying more systematic or mathematical structures of two-body or many-body quantum states. Thus, a better understanding of quantum geometry in many-body systems and the corresponding physical consequences remains intended [85–87].

ACKNOWLEDGMENTS

The author is grateful to Ryuichi Shindou for his fruitful suggestions and support. The author also thanks Lingxian Kong, Zhenyu Xiao, Xuesong Hu, Pengwei Zhao, and Siyu Pan for their helpful discussions. The work was supported by the National Basic Research Programs of China (Grant No. 2019YFA0308401) and the National Natural Science Foundation of China (Grants No. 11674011 and No. 12074008).

APPENDIX A: DERIVATION OF THE SECOND-ORDER EFFECTIVE INTERACTION

In this Appendix, we derive the second-order effective interaction [Eqs. (15)–(17)] in Sec. A 1 and the form after the gauge transformation [Eq. (18)] in Sec. A 2. We denote

$$\frac{2}{g}H_{I2} \equiv \frac{1}{(2\pi)^d}\int_\infty \left(\prod_{i=1}^3 d^d\boldsymbol{k}_i\right) b^\dagger_{\boldsymbol{k}_1} b^\dagger_{\boldsymbol{k}_2} b_{\boldsymbol{k}_3} b_{\boldsymbol{k}_4} F_2(\boldsymbol{k}_1,\boldsymbol{k}_2,\boldsymbol{k}_3,\boldsymbol{k}_4). \tag{A1}$$

We define three independent momenta, respectively, representing the Cooper, direct, and exchange channels,

$$\boldsymbol{s} \equiv \boldsymbol{k}_1 + \boldsymbol{k}_2, \quad \boldsymbol{t} \equiv \boldsymbol{k}_3 - \boldsymbol{k}_1, \quad \boldsymbol{u} \equiv \boldsymbol{k}_3 - \boldsymbol{k}_2. \tag{A2}$$

1. Momentum expansion and Fourier transform

Second-order terms in $\langle\langle u_{\boldsymbol{k}_1} u_{\boldsymbol{k}_2} | u_{\boldsymbol{k}_3} u_{\boldsymbol{k}_4}\rangle\rangle$ read

$$\begin{aligned} F_2(\boldsymbol{k}_1,\boldsymbol{k}_2,\boldsymbol{k}_3,\boldsymbol{k}_4) = {}& \tfrac{1}{2}\left\langle\left\langle u\partial_{k_\alpha}\partial_{k_\beta}u\middle|uu\right\rangle\right\rangle_{\boldsymbol{0}}(k_{1\alpha}k_{1\beta} + k_{2\alpha}k_{2\beta}) \\ & + \tfrac{1}{2}\left\langle\left\langle uu\middle|u\partial_{k_\alpha}\partial_{k_\beta}u\right\rangle\right\rangle_{\boldsymbol{0}}(k_{3\alpha}k_{3\beta} + k_{4\alpha}k_{4\beta}) \\ & + \left\langle\left\langle\left(\partial_{k_\alpha}u\right)\left(\partial_{k_\beta}u\right)\middle|uu\right\rangle\right\rangle_{\boldsymbol{0}}k_{1\alpha}k_{2\beta} \\ & + \left\langle\left\langle uu\middle|\left(\partial_{k_\alpha}u\right)\left(\partial_{k_\beta}u\right)\right\rangle\right\rangle_{\boldsymbol{0}}k_{3\alpha}k_{4\beta} \\ & + \left\langle\left\langle u\partial_{k_\alpha}u\middle|u\partial_{k_\beta}u\right\rangle\right\rangle_{\boldsymbol{0}}(k_{1\alpha}+k_{2\alpha})(k_{3\beta}+k_{4\beta}). \end{aligned} \tag{A3}$$

With momentum conservation, we get

$$\begin{aligned} & F_2(\boldsymbol{k}_1,\boldsymbol{k}_2,\boldsymbol{k}_3,\boldsymbol{k}_4)|_{\boldsymbol{k}_4=\boldsymbol{k}_1+\boldsymbol{k}_2-\boldsymbol{k}_3} \\ & = \tfrac{1}{4}\left(\left\langle\left\langle uu\middle|\left(\partial_{k_\alpha}u\right)\left(\partial_{k_\beta}u\right)\right\rangle\right\rangle_{\boldsymbol{0}} + \left\langle\left\langle uu\middle|u\partial_{k_\alpha}\partial_{k_\beta}u\right\rangle\right\rangle_{\boldsymbol{0}}\right. \\ & \quad \left. + \left\langle\left\langle u\partial_{k_\alpha}u\middle|u\partial_{k_\beta}u\right\rangle\right\rangle_{\boldsymbol{0}} + \left\langle\left\langle u\partial_{k_\beta}u\middle|u\partial_{k_\alpha}u\right\rangle\right\rangle_{\boldsymbol{0}} + \text{c.c.}\right)s_\alpha s_\beta \end{aligned}$$

$$+\tfrac{1}{4}\big(\langle\langle uu|u\partial_{k_\alpha}\partial_{k_\beta}u\rangle\rangle_{\mathbf{0}}-\langle\langle uu|(\partial_{k_\alpha}u)(\partial_{k_\beta}u)\rangle\rangle_{\mathbf{0}}+\text{c.c.}\big)(t_\alpha t_\beta+u_\alpha u_\beta)$$
$$+\tfrac{1}{4}\big(\langle\langle uu|u\partial_{k_\alpha}\partial_{k_\beta}u\rangle\rangle_{\mathbf{0}}-\langle\langle uu|(\partial_{k_\alpha}u)(\partial_{k_\beta}u)\rangle\rangle_{\mathbf{0}}-\text{c.c.}\big)(t_\alpha u_\beta+u_\alpha t_\beta),\tag{A4}$$

where we have used

$$\boldsymbol{k}_1-\boldsymbol{k}_2=(\boldsymbol{k}_3-\boldsymbol{k}_2)-(\boldsymbol{k}_3-\boldsymbol{k}_1),\tag{A5}$$

$$\boldsymbol{k}_3-\boldsymbol{k}_4=(\boldsymbol{k}_3-\boldsymbol{k}_1)+(\boldsymbol{k}_1-\boldsymbol{k}_4)=(\boldsymbol{k}_3-\boldsymbol{k}_1)+(\boldsymbol{k}_3-\boldsymbol{k}_2).\tag{A6}$$

Note that the direct channel and the exchange channel are symmetric.

Because $\langle\langle uu|uu\rangle\rangle_{\boldsymbol{k}}\equiv\langle\langle u_{\boldsymbol{k}}u_{\boldsymbol{k}}|u_{\boldsymbol{k}}u_{\boldsymbol{k}}\rangle\rangle$ is not a constant, we have two gauge-independent quantities characterizing momentum dependence,

$$\partial_{k_\alpha}\langle\langle uu|uu\rangle\rangle_{\boldsymbol{k}}=2\langle\langle u\partial_{k_\alpha}u|uu\rangle\rangle_{\boldsymbol{k}}+2\langle\langle uu|u\partial_{k_\alpha}u\rangle\rangle_{\boldsymbol{k}},\tag{A7}$$

$$\begin{aligned}&\partial_{k_\alpha}\partial_{k_\beta}\langle\langle uu|uu\rangle\rangle_{\boldsymbol{k}}\\&=4\langle\langle u\partial_{k_\alpha}u|u\partial_{k_\beta}u\rangle\rangle_{\boldsymbol{k}}+2\langle\langle(\partial_{k_\alpha}u)(\partial_{k_\beta}u)|uu\rangle\rangle_{\boldsymbol{k}}\\&\quad+2\langle\langle u\partial_{k_\alpha}\partial_{k_\beta}u|uu\rangle\rangle_{\boldsymbol{k}}+4\langle\langle u\partial_{k_\beta}u|u\partial_{k_\alpha}u\rangle\rangle_{\boldsymbol{k}}\\&\quad+2\langle\langle uu|(\partial_{k_\alpha}u)(\partial_{k_\beta}u)\rangle\rangle_{\boldsymbol{k}}+2\langle\langle uu|u\partial_{k_\alpha}\partial_{k_\beta}u\rangle\rangle_{\boldsymbol{k}}.\end{aligned}\tag{A8}$$

In addition, we can apply derivatives on $|u_{\boldsymbol{k}}|^2$ to construct a gauge-independent quantity,

$$\begin{aligned}&\langle\langle\partial_{k_\alpha}(u^*u)|\partial_{k_\beta}(u^*u)\rangle\rangle_{\boldsymbol{k}}\\&\equiv\frac{(2\pi)^{2d}}{\Omega_{\text{cell}}}\int d^d\boldsymbol{r}\,\partial_{k_\alpha}[u^*_{\boldsymbol{k}}(\boldsymbol{r})u_{\boldsymbol{k}}(\boldsymbol{r})]\partial_{k_\beta}[u^*_{\boldsymbol{k}}(\boldsymbol{r})u_{\boldsymbol{k}}(\boldsymbol{r})]\\&=\langle\langle u\partial_{k_\alpha}u|u\partial_{k_\beta}u\rangle\rangle_{\boldsymbol{k}}+\langle\langle u\partial_{k_\beta}u|u\partial_{k_\alpha}u\rangle\rangle_{\boldsymbol{k}}\\&\quad+\langle\langle(\partial_{k_\alpha}u)(\partial_{k_\beta}u)|uu\rangle\rangle_{\boldsymbol{k}}+\langle\langle uu|(\partial_{k_\alpha}u)(\partial_{k_\beta}u)\rangle\rangle_{\boldsymbol{k}}.\end{aligned}\tag{A9}$$

Then two of the terms in Eq. (A4) are gauge independent,

$$\begin{aligned}&F_2(\boldsymbol{k}_1,\boldsymbol{k}_2,\boldsymbol{k}_3,\boldsymbol{k}_4)|_{\boldsymbol{k}_4=\boldsymbol{k}_1+\boldsymbol{k}_2-\boldsymbol{k}_3}\\&=\frac{1}{8}M''_{\alpha\beta}(\mathbf{0})s_\alpha s_\beta+\frac{1}{8}[M''_{\alpha\beta}(\mathbf{0})-4P_{\alpha\beta}(\mathbf{0})](t_\alpha t_\beta+u_\alpha u_\beta)\\&\quad+\frac{i}{2}\widetilde{S}_{\alpha\beta}(\mathbf{0})(t_\alpha u_\beta+u_\alpha t_\beta).\end{aligned}\tag{A10}$$

We can further express H_{I2} in the real space with the hydrodynamic variables. With

$$b(\boldsymbol{r})=\int_\infty\frac{d^d\boldsymbol{k}}{(2\pi)^{\frac{d}{2}}}b_{\boldsymbol{k}}e^{i\boldsymbol{k}\cdot\boldsymbol{r}},\tag{A11}$$

we get

$$\begin{aligned}&\frac{1}{(2\pi)^d}\int_\infty\left(\prod_{i=1}^3d^d\boldsymbol{k}_i\right)b^\dagger_{\boldsymbol{k}_1}b^\dagger_{\boldsymbol{k}_2}b_{\boldsymbol{k}_3}b_{\boldsymbol{k}_4}\frac{1}{8}M''_{\alpha\beta}(\mathbf{0})s_\alpha s_\beta\\&=\int_\infty d^d\boldsymbol{r}\frac{1}{8}M''_{\alpha\beta}(\mathbf{0})[\partial_\alpha(b^\dagger b^\dagger)][\partial_\beta(bb)]\\&=\int_\infty d^d\boldsymbol{r}\frac{1}{8}M''_{\alpha\beta}(\mathbf{0})[(\partial_\alpha n)(\partial_\beta n)+4n^2(\partial_\alpha\theta)(\partial_\beta\theta)],\end{aligned}\tag{A12}$$

$$\begin{aligned}&\frac{1}{(2\pi)^d}\int_\infty\left(\prod_{i=1}^3d^d\boldsymbol{k}_i\right)b^\dagger_{\boldsymbol{k}_1}b^\dagger_{\boldsymbol{k}_2}b_{\boldsymbol{k}_3}b_{\boldsymbol{k}_4}\frac{1}{8}[M''_{\alpha\beta}(\mathbf{0})-4P_{\alpha\beta}(\mathbf{0})](t_\alpha t_\beta+u_\alpha u_\beta)\\&=\int_\infty d^d\boldsymbol{r}\frac{1}{4}[M''_{\alpha\beta}(\mathbf{0})-4P_{\alpha\beta}(\mathbf{0})][\partial_\alpha(b^\dagger b)][\partial_\beta(b^\dagger b)]\\&=\int_\infty d^d\boldsymbol{r}\left[\frac{1}{4}M''_{\alpha\beta}(\mathbf{0})-P_{\alpha\beta}(\mathbf{0})\right](\partial_\alpha n)(\partial_\beta n),\end{aligned}\tag{A13}$$

$$\begin{aligned}&\frac{1}{(2\pi)^d}\int_\infty\left(\prod_{i=1}^3d^d\boldsymbol{k}_i\right)b^\dagger_{\boldsymbol{k}_1}b^\dagger_{\boldsymbol{k}_2}b_{\boldsymbol{k}_3}b_{\boldsymbol{k}_4}\left[\frac{i}{2}\widetilde{S}_{\alpha\beta}(\mathbf{0})\right](t_\alpha u_\beta+u_\alpha t_\beta)\\&=\int_\infty d^d\boldsymbol{r}\widetilde{S}_{\alpha\beta}(\mathbf{0})\frac{i}{2}[b^\dagger(\partial_\alpha\partial_\beta b^\dagger)bb-(\partial_\alpha b^\dagger)(\partial_\beta b^\dagger)bb\\&\quad-b^\dagger b^\dagger b(\partial_\alpha\partial_\beta b)+b^\dagger b^\dagger(\partial_\alpha b)(\partial_\beta b)]\\&=-2\int_\infty d^d\boldsymbol{r}\widetilde{S}_{\alpha\beta}(\mathbf{0})n(\partial_\alpha n)(\partial_\beta\theta).\end{aligned}\tag{A14}$$

When deriving Eq. (A14), we have used

$$\tfrac{1}{2}(t_\alpha u_\beta+u_\alpha t_\beta)=-\tfrac{1}{4}[(k_{1\alpha}-k_{2\alpha})(k_{1\beta}-k_{2\beta})-(k_{3\alpha}-k_{4\alpha})(k_{3\beta}-k_{4\beta})],\tag{A15}$$

$$b^\dagger(\partial_\alpha\partial_\beta b^\dagger)bb-(\partial_\alpha b^\dagger)(\partial_\beta b^\dagger)bb=n^{\frac{3}{2}}\partial_\alpha\partial_\beta n^{\frac{1}{2}}-n\big(\partial_\alpha n^{\frac{1}{2}}\big)\big(\partial_\beta n^{\frac{1}{2}}\big)-in^2\partial_\alpha\partial_\beta\theta.\tag{A16}$$

Equations (A1), (A10), and (A12)–(A14) are consistent with Eqs. (15)–(17).

2. Gauge transformation

Under the gauge transformation,

$$u_{\boldsymbol{k}}\to\tilde{u}_{\boldsymbol{k}}\equiv u_{\boldsymbol{k}}e^{i\vartheta_{\boldsymbol{k}}},\tag{A17}$$

$\widetilde{S}(\boldsymbol{k})$ is changed,

$$\begin{aligned}&\langle\langle\tilde{u}\tilde{u}|\tilde{u}\partial_{k_\alpha}\partial_{k_\beta}\tilde{u}\rangle\rangle_{\boldsymbol{k}}-\langle\langle\tilde{u}\tilde{u}|(\partial_{k_\alpha}\tilde{u})(\partial_{k_\beta}\tilde{u})\rangle\rangle_{\boldsymbol{k}}-\text{c.c.}\\&=\langle\langle uu|ue^{-i\vartheta}\partial_{k_\alpha}\big[(\partial_{k_\beta}u)e^{i\vartheta}+i(\partial_{k_\beta}\vartheta)ue^{i\vartheta}\big]\rangle\rangle_{\boldsymbol{k}}\\&\quad-\langle\langle uu|\big[\partial_{k_\alpha}u+i(\partial_{k_\alpha}\vartheta)u\big]\big[\partial_{k_\beta}u+i(\partial_{k_\beta}\vartheta)u\big]\rangle\rangle_{\boldsymbol{k}}-\text{c.c.}\\&=\langle\langle uu|u\partial_{k_\alpha}\partial_{k_\beta}u\rangle\rangle_{\boldsymbol{k}}-\langle\langle uu|(\partial_{k_\alpha}u)(\partial_{k_\beta}u)\rangle\rangle_{\boldsymbol{k}}\\&\quad+i(\partial_{k_\alpha}\partial_{k_\beta}\vartheta)\langle\langle uu|uu\rangle\rangle_{\boldsymbol{k}}-\text{c.c.}\end{aligned}\tag{A18}$$

With the gauge given by Eq. (8), we get

$$\begin{aligned}&\langle\langle\tilde{u}\tilde{u}|\tilde{u}\partial_{k_\alpha}\partial_{k_\beta}\tilde{u}\rangle\rangle_{\mathbf{0}}-\langle\langle\tilde{u}\tilde{u}|(\partial_{k_\alpha}\tilde{u})(\partial_{k_\beta}\tilde{u})\rangle\rangle_{\mathbf{0}}-\text{c.c.}\\&=\langle\langle uu|u\partial_{k_\alpha}\partial_{k_\beta}u\rangle\rangle_{\mathbf{0}}-\langle\langle uu|(\partial_{k_\alpha}u)(\partial_{k_\beta}u)\rangle\rangle_{\mathbf{0}}\\&\quad+\frac{i}{2}\langle\langle uu|uu\rangle\rangle_{\mathbf{0}}\big[\partial_{k_\alpha}A_\beta(\mathbf{0})+\partial_{k_\beta}A_\alpha(\mathbf{0})\big]-\text{c.c.}\\&=\langle\langle uu|u\partial_{k_\alpha}\partial_{k_\beta}u\rangle\rangle_{\mathbf{0}}-\langle\langle uu|(\partial_{k_\alpha}u)(\partial_{k_\beta}u)\rangle\rangle_{\mathbf{0}}\\&\quad-\frac{1}{2}\langle\langle uu|uu\rangle\rangle_{\mathbf{0}}\big(\partial_{k_\alpha}\langle u|\partial_{k_\beta}u\rangle_{\mathbf{0}}+\partial_{k_\beta}\langle u|\partial_{k_\alpha}u\rangle_{\mathbf{0}}\big)-\text{c.c.}\\&=\langle\langle uu|u\partial_{k_\alpha}\partial_{k_\beta}u\rangle\rangle_{\mathbf{0}}-\langle\langle uu|(\partial_{k_\alpha}u)(\partial_{k_\beta}u)\rangle\rangle_{\mathbf{0}}\\&\quad-\langle\langle uu|uu\rangle\rangle_{\mathbf{0}}\langle u|\partial_{k_\alpha}\partial_{k_\beta}u\rangle_{\mathbf{0}}-\text{c.c.}\end{aligned}\tag{A19}$$

So, $\widetilde{S}_{\alpha\beta}(\mathbf{0})$ in Eq. (15) should be substituted by $S_{\alpha\beta}(\mathbf{0})$ defined in Eq. (18). We can also verify that $S_{\alpha\beta}(\boldsymbol{k})$ is gauge independent,

$$\begin{aligned}
&\langle\!\langle \tilde{u}\tilde{u}|\tilde{u}\partial_{k_\alpha}\partial_{k_\beta}\tilde{u}\rangle\!\rangle_{\boldsymbol{k}} - \langle\!\langle \tilde{u}\tilde{u}|(\partial_{k_\alpha}\tilde{u})(\partial_{k_\beta}\tilde{u})\rangle\!\rangle_{\boldsymbol{k}} \\
&\quad + \frac{i}{2}\langle\langle \tilde{u}\tilde{u}|\tilde{u}\tilde{u}\rangle\rangle_{\boldsymbol{k}}[\partial_\alpha\tilde{A}_\beta(\boldsymbol{k}) + \partial_\beta\tilde{A}_\alpha(\boldsymbol{k})] \\
&= \langle\!\langle uu|u\partial_{k_\alpha}\partial_{k_\beta}u\rangle\!\rangle_{\boldsymbol{k}} - \langle\!\langle uu|\partial_{k_\alpha}u\partial_{k_\beta}u\rangle\!\rangle_{\boldsymbol{k}} \\
&\quad + i\partial_{k_\alpha}\partial_{k_\beta}\vartheta(\boldsymbol{k})\langle\langle uu|uu\rangle\rangle_{\boldsymbol{k}} + \frac{i}{2}\langle\langle uu|uu\rangle\rangle_{\boldsymbol{k}}\big[\partial_{k_\alpha}A_\beta(\boldsymbol{k}) \\
&\quad - \partial_{k_\alpha}\partial_{k_\beta}\vartheta(\boldsymbol{k}) + \partial_{k_\beta}A_\alpha(\boldsymbol{k}) - \partial_{k_\alpha}\partial_{k_\beta}\vartheta(\boldsymbol{k})\big] \\
&= \langle\!\langle uu|u\partial_{k_\alpha}\partial_{k_\beta}u\rangle\!\rangle_{\boldsymbol{k}} - \langle\!\langle uu|\partial_{k_\alpha}u\partial_{k_\beta}u\rangle\!\rangle_{\boldsymbol{k}} \\
&\quad + \frac{i}{2}\langle\langle uu|uu\rangle\rangle_{\boldsymbol{k}}\big[\partial_{k_\alpha}A_\beta(\boldsymbol{k}) + \partial_{k_\beta}A_\alpha(\boldsymbol{k})\big],
\end{aligned} \tag{A20}$$

where $\tilde{A}_\alpha(\boldsymbol{k}) \equiv i\langle\tilde{u}|\partial_{k_\alpha}\tilde{u}\rangle_{\boldsymbol{k}}$.

APPENDIX B: SOLUTIONS OF COLLECTIVE MODES IN A HARMONIC TRAP

In this Appendix, we solve the linear homogeneous ordinary differential equations (38) and (40) with proper boundary conditions to get the low-energy collective modes in the harmonic trap. We first take $\eta = 0$ to review the results without the optical lattice in Sec. B 1. The general case of $\eta \neq 0$ is solved in Sec. B 2. Obvious differences can be seen by a comparison of the two cases. In addition, we prove the orthonormal relation given by Eq. (43) in Sec. B 3. We omit the subscripts of $\rho_{\mathsf{n,j}}$ and $\omega_{\mathsf{n,j}}$ when there is no ambiguity and denote $\kappa = \frac{\omega^2}{\omega_0^2}$.

1. Without lattice-induced wave-function effects

a. 3D case

When $\eta = 0$, Eq. (38) becomes

$$\begin{aligned}
&\frac{1}{2}(1-r^2)\frac{d^2\rho}{dr^2} + (1-2r^2)\frac{1}{r}\frac{d\rho}{dr} \\
&\quad + \left[\kappa - (1-r^2)\frac{\ell(\ell+1)}{2r^2}\right]\rho = 0.
\end{aligned} \tag{B1}$$

When $r \to 0$, we get

$$\frac{1}{2}\frac{d^2\rho}{dr^2} + \frac{1}{r}\frac{d\rho}{dr} - \frac{\ell(\ell+1)}{2r^2}\rho = 0. \tag{B2}$$

Taking $\rho = r^l$ into Eq. (B2), we get $l(l+1) = \ell(\ell+1)$, so $l = \ell$ or $l = -\ell - 1$. Because $\ell \in \mathbb{N}$, to make $\rho(r)$ finite when $r \to 0$, we take $l = \ell$. Suppose an eigenfunction is a polynomial,

$$\rho(r) = \sum_{\mathsf{k}'=0}^{\mathsf{N}'} \alpha_{\mathsf{k}'} r^{\mathsf{k}'+\ell}, \tag{B3}$$

and we get

$$\begin{aligned}
&\sum_{\mathsf{k}'=-2}^{\mathsf{N}'-2} \alpha_{\mathsf{k}'+2}\left[\frac{1}{2}(\ell+\mathsf{k}'+2)(\ell+\mathsf{k}'+1)\right. \\
&\qquad \left. + (\ell+\mathsf{k}'+2) - \frac{1}{2}\ell(\ell+1)\right] r^{\ell+\mathsf{k}'} \\
&= \sum_{\mathsf{k}=0}^{\mathsf{N}'} \alpha_{\mathsf{k}'}\left[\frac{1}{2}(\ell+\mathsf{k}')(\ell+\mathsf{k}'-1)\right. \\
&\qquad \left. + 2(\ell+\mathsf{k}') - \kappa - \frac{1}{2}\ell(\ell+1)\right] r^{\ell+\mathsf{k}'}.
\end{aligned} \tag{B4}$$

An equation for $r^{\ell-2}$ is automatically satisfied because it is equivalent to the asymptotic equation (B2). Equations for $r^{\ell+2\mathsf{k}'-1}$ ($\mathsf{k}' \in \mathbb{N}$) require k' and N' to be even numbers, so we can denote $\mathsf{k}' = 2\mathsf{k}$, $\mathsf{N}' = 2\mathsf{N}$. Equations for $r^{\ell+2\mathsf{k}}$ ($0 < \mathsf{k} < \mathsf{N}$, $\mathsf{k} \in \mathbb{N}$) give a recursion condition,

$$\begin{aligned}
&\alpha_{2\mathsf{k}+2}\left[\tfrac{1}{2}(\ell+2\mathsf{k}+2)(\ell+2\mathsf{k}+1) + (\ell+2\mathsf{k}+2)\right. \\
&\qquad \left. - \tfrac{1}{2}\ell(\ell+1)\right] = \alpha_{2\mathsf{k}}\left[\tfrac{1}{2}(\ell+2\mathsf{k})(\ell+2\mathsf{k}-1)\right. \\
&\qquad \left. + 2(\ell+2\mathsf{k}) - \kappa - \tfrac{1}{2}\ell(\ell+1)\right].
\end{aligned} \tag{B5}$$

When N is finite, $\mathsf{N} = \mathsf{n}$ and an equation for $r^{\ell+2\mathsf{n}}$ gives

$$\begin{aligned}
\kappa &= \tfrac{1}{2}(\ell+2\mathsf{n})(\ell+2\mathsf{n}-1) + 2(\ell+2\mathsf{n}) - \tfrac{1}{2}\ell(\ell+1) \\
&= 2\mathsf{n}^2 + 2\mathsf{n}\ell + 3\mathsf{n} + \ell.
\end{aligned} \tag{B6}$$

Taking Eq. (B6) into Eq. (B5), we have

$$\alpha_{2\mathsf{k}+2} = -\frac{(\mathsf{n}-\mathsf{k})(2\mathsf{k}+2\mathsf{n}+2\ell+3)}{(\mathsf{k}+1)(2\mathsf{k}+2\ell+3)}\alpha_{2\mathsf{k}}. \tag{B7}$$

Below we explain why we cannot take $\mathsf{N} = \infty$. In this case, when $\mathsf{k} \to \infty$, Eq. (B5) gives

$$\frac{\alpha_{2\mathsf{k}+2}}{\alpha_{2\mathsf{k}}} = \frac{2+\frac{2\ell+3}{\mathsf{k}}}{2+\frac{2\ell+5}{\mathsf{k}}} + O\left(\frac{1}{\mathsf{k}^2}\right) = 1 - \frac{1}{\mathsf{k}} + O\left(\frac{1}{\mathsf{k}^2}\right). \tag{B8}$$

We can take a test form of $\alpha_{2\mathsf{k}}$ for $\mathsf{k} \to \infty$,

$$\alpha_{2\mathsf{k}} = \frac{C}{\mathsf{k}^\zeta}\left(1 + \frac{C'}{\mathsf{k}^{\zeta'}}\right), \tag{B9}$$

where $\zeta > 0$, $\zeta' > 0$, and C and C' are constant; then

$$\begin{aligned}
\frac{\alpha_{2\mathsf{k}+2}}{\alpha_{2\mathsf{k}}} &= \frac{\mathsf{k}^\zeta}{(\mathsf{k}+1)^\zeta}\frac{1+\frac{C'}{(\mathsf{k}+1)^{\zeta'}}}{1+\frac{C'}{\mathsf{k}^{\zeta'}}} \\
&= \left(1-\frac{\zeta}{\mathsf{k}}\right)\left[1+\frac{C'}{(\mathsf{k}+1)^{\zeta'}}\right]\left(1-\frac{C'}{\mathsf{k}^{\zeta'}}\right) \\
&\quad + O\left(\frac{1}{\mathsf{k}^{\zeta'+1}}\right) + O\left(\frac{1}{\mathsf{k}^2}\right) \\
&= 1 - \frac{\zeta}{\mathsf{k}} + O\left(\frac{1}{\mathsf{k}^{\zeta'+1}}\right) + O\left(\frac{1}{\mathsf{k}^2}\right).
\end{aligned} \tag{B10}$$

Comparing Eq. (B10) with Eq. (B8), we get $\zeta = 1$. Equation (B9) can be generalized to show that $\alpha_{2\mathsf{k}} = \frac{C}{\mathsf{k}} + O(\frac{1}{\mathsf{k}^2})$.

Then we get

$$\rho(r\to 1)=\sum_{\mathsf{k}=0}^{\mathsf{k}_0}\alpha_{2\mathsf{k}}+\sum_{\mathsf{k}=\mathsf{k}_0}^{\infty}\left[\frac{C}{\mathsf{k}}+O\left(\frac{1}{\mathsf{k}^2}\right)\right]\to\infty, \quad \text{(B11)}$$

where k_0 is a constant that is large enough. It is unphysical to have a divergent $\rho_{\mathsf{n},\ell}$ when $r\to 1$. Note that at least one of n and ℓ is nonzero in the divergent case, so $n(\boldsymbol{r},t)$ becomes negative for some spacetime coordinates. To avoid the divergence, we need Eq. (B6) to truncate the sequence α_{2k} and get a finite N.

In summary, eigenfunctions take a form

$$\rho_{\mathsf{n},\ell}=\sum_{\mathsf{k}=0}^{\mathsf{N}}\alpha_{\mathsf{n},\ell,2\mathsf{k}}r^{2\mathsf{k}+\ell}, \quad \text{(B12)}$$

where $\alpha_{\mathsf{n},\ell,2\mathsf{k}}$ satisfies Eq. (B7). When $\eta=0$, we get $\mathsf{N}=\mathsf{n}$ in Eq. (B12), but we will show that this is not true for $\eta\neq 0$.

b. 2D case

When $\eta=0$, Eq. (40) becomes

$$\frac{1}{2}(1-r^2)\frac{d^2\rho}{dr^2}+\frac{1}{2}(1-3r^2)\frac{1}{r}\frac{d\rho}{dr}+\left[\kappa r^2-\frac{1}{2}\mathsf{m}^2(1-r^2)\right]\frac{\rho}{r^2}=0. \quad \text{(B13)}$$

An analysis of $r\to 0$ gives $\rho(r\to 0)\to r^{|\mathsf{m}|}$; then we get

$$\rho_{\mathsf{n},|\mathsf{m}|}=\sum_{\mathsf{k}=0}^{\mathsf{N}}\alpha_{\mathsf{n},|\mathsf{m}|,2\mathsf{k}}r^{2\mathsf{k}+|\mathsf{m}|}. \quad \text{(B14)}$$

Let us take $\mathsf{m}\geqslant 0$ for simplicity. There is a recursion relation,

$$\begin{aligned}&\alpha_{2\mathsf{k}+2}\left[\tfrac{1}{2}(\mathsf{m}+2\mathsf{k}+2)(\mathsf{m}+2\mathsf{k}+1)+\tfrac{1}{2}(\mathsf{m}+2\mathsf{k}+2)-\tfrac{1}{2}\mathsf{m}^2\right]\\&=\alpha_{2\mathsf{k}}\left[\tfrac{1}{2}(\mathsf{m}+2\mathsf{k})(\mathsf{m}+2\mathsf{k}-1)+\tfrac{3}{2}(\mathsf{m}+2\mathsf{k})-\kappa-\tfrac{1}{2}\mathsf{m}^2\right]. \quad \text{(B15)}\end{aligned}$$

If N is finite, we get $\mathsf{N}=\mathsf{n}$ and

$$\begin{aligned}\kappa&=\frac{1}{2}(\mathsf{m}+2\mathsf{n})(\mathsf{m}+2\mathsf{n}-1)+\frac{3}{2}(\mathsf{m}+2\mathsf{n})-\frac{1}{2}\mathsf{m}^2\\&=2\mathsf{n}^2+2\mathsf{n}\mathsf{m}+2\mathsf{n}+\mathsf{m}, \quad \text{(B16)}\end{aligned}$$

$$\begin{aligned}\alpha_{2\mathsf{k}+2}&=\alpha_{2\mathsf{k}}\frac{2(\mathsf{k}-\mathsf{n})(\mathsf{k}+\mathsf{n})+2(\mathsf{k}-\mathsf{n})(\mathsf{m}+1)}{\frac{1}{2}(\mathsf{m}+2\mathsf{k}+2)^2-\frac{1}{2}\mathsf{m}^2}\\&=\alpha_{2\mathsf{k}}\frac{(\mathsf{k}-\mathsf{n})(\mathsf{k}+\mathsf{n}+\mathsf{m}+1)}{(\mathsf{k}+1)(\mathsf{k}+\mathsf{m}+1)}. \quad \text{(B17)}\end{aligned}$$

If $\mathsf{N}=\infty$, then when $\mathsf{k}\to\infty$, we get

$$\begin{aligned}\frac{\alpha_{2\mathsf{k}+2}}{\alpha_{2\mathsf{k}}}&=\frac{2\mathsf{k}^2+(2\mathsf{m}+2)\mathsf{k}}{2\mathsf{k}^2+(2\mathsf{m}+4)\mathsf{k}}+O\left(\frac{1}{\mathsf{k}^2}\right)\\&=1-\frac{1}{\mathsf{k}}+O\left(\frac{1}{\mathsf{k}^2}\right), \quad \text{(B18)}\end{aligned}$$

and by the analysis below Eq. (B8), we know it is impossible.

2. With lattice-induced wave-function effects

a. 3D case

Consider Eq. (38) with $\eta\neq 0$. Note that η can be an $O(1)$ quantity. We have an equation,

$$\begin{aligned}&\frac{1}{2}\left[\left(1+\frac{\eta}{2}\right)-(1+\eta)r^2+\frac{\eta}{2}r^4\right]\frac{d^2\rho}{dr^2}\\&+\left[\left(1+\frac{\eta}{2}\right)-2(1+\eta)r^2+\frac{3\eta}{2}r^4\right]\frac{1}{r}\frac{d\rho}{dr}\\&+\left\{\kappa r^2-\frac{1}{2}\ell(\ell+1)\left[\left(1+\frac{\eta}{2}\right)-(1+\eta)r^2+\frac{\eta}{2}r^4\right]\right\}\frac{\rho}{r^2}=0. \quad \text{(B19)}\end{aligned}$$

When $r\to 0$, we get

$$\frac{1}{2}\left(1+\frac{\eta}{2}\right)\frac{d^2\rho}{dr^2}+\left(1+\frac{\eta}{2}\right)\frac{1}{r}\frac{d\rho}{dr}-\frac{1}{2}\ell(\ell+1)\left(1+\frac{\eta}{2}\right)\frac{\rho}{r^2}=0. \quad \text{(B20)}$$

Equation (B20) is identical to Eq. (B2). Then we can take Eq. (B12) into Eq. (B19), and the difference from before is that we will get a second-order recursion relation, i.e., $\alpha_{2\mathsf{k}+2}$ should be determined by $\alpha_{2\mathsf{k}}$ and $\alpha_{2\mathsf{k}-2}$,

$$\begin{aligned}&\sum_{\mathsf{k}=-1}^{\mathsf{N}-1}\alpha_{2\mathsf{k}+2}\left[\frac{1}{2}\left(1+\frac{\eta}{2}\right)(\ell+2\mathsf{k}+2)(\ell+2\mathsf{k}+1)\right.\\&\left.+\left(1+\frac{\eta}{2}\right)(\ell+2\mathsf{k}+2)-\frac{1}{2}\left(1+\frac{\eta}{2}\right)\ell(\ell+1)\right]r^{\ell+2\mathsf{k}}\\&+\sum_{\mathsf{k}=0}^{\mathsf{N}}\alpha_{2\mathsf{k}}\left[-\frac{1}{2}(1+\eta)(\ell+2\mathsf{k})(\ell+2\mathsf{k}-1)\right.\\&\left.-2(1+\eta)(\ell+2\mathsf{k})+\kappa+\frac{1}{2}(1+\eta)\ell(\ell+1)\right]r^{\ell+2\mathsf{k}}\\&+\sum_{\mathsf{k}=1}^{\mathsf{N}+1}\alpha_{2\mathsf{k}-2}\left[\frac{\eta}{4}(\ell+2\mathsf{k}-2)(\ell+2\mathsf{k}-3)\right.\\&\left.+\frac{3}{2}\eta(\ell+2\mathsf{k}-2)-\frac{\eta}{4}\ell(\ell+1)\right]r^{\ell+2\mathsf{k}}=0. \quad \text{(B21)}\end{aligned}$$

However, if N is finite, an equation for $\alpha_{2\mathsf{N}}r^{\ell+2\mathsf{N}+2}$ gives

$$\begin{aligned}&\tfrac{1}{4}(\ell+2\mathsf{N})(\ell+2\mathsf{N}-1)+\tfrac{3}{2}(\ell+2\mathsf{N})-\tfrac{1}{4}\ell(\ell+1)\\&=(\mathsf{N}+1)\ell+\tfrac{1}{2}\mathsf{N}(2\mathsf{N}+5)=0, \quad \text{(B22)}\end{aligned}$$

whose only solution is $\mathsf{N}=\ell=0$, and an equation for $\alpha_{2\mathsf{N}}r^{\ell+2\mathsf{N}}$ gives $\kappa=0$. Except for this trivial zero mode (δn is a constant), we should take $\mathsf{N}=\infty$.

When $\mathsf{N}=\infty$ and $\mathsf{k}\to\infty$, we can apply an expansion of k^{-1}. At the leading order, we get a recursion relation,

$$(2+\eta)\alpha_{2\mathsf{k}+2}-2(1+\eta)\alpha_{2\mathsf{k}}+\eta\alpha_{2\mathsf{k}-2}=0, \quad \text{(B23)}$$

which leads to

$$\alpha_{2\mathsf{k}}=A_1+A_2\left(\frac{\eta}{2+\eta}\right)^{\mathsf{k}}. \quad \text{(B24)}$$

So there are two parts of $\alpha_{2\mathsf{k}}$ with different decay exponents. Let us concentrate on the case of $\eta > -1$ so that $|\frac{\eta}{2+\eta}| < 1$. At the next-to-leading order, similar to Eq. (B9), A_1 and A_2 in Eq. (B24) are no longer constants but proportional to powers of k. Because Eq. (B23) is linear, we can solve A_1 and A_2 separately, namely, we can take only one of them to be nonzero. Taking $\alpha_{2\mathsf{k}} = \frac{C_1}{\mathsf{k}^{\zeta_1}}$, we get

$$\left(1-\frac{\zeta_1}{\mathsf{k}}\right)\left(1+\frac{\eta}{2}\right)\left(1+\frac{2\ell+5}{2\mathsf{k}}\right)-(1+\eta)\left(1+\frac{2\ell+3}{2\mathsf{k}}\right)+\left(1+\frac{\zeta_1}{\mathsf{k}}\right)\frac{\eta}{2}\left(1+\frac{2\ell+1}{2\mathsf{k}}\right)+O\left(\frac{1}{\mathsf{k}^2}\right)=0, \tag{B25}$$

so the power ζ_1 is determined,

$$\zeta_1=\left(1+\frac{\eta}{2}\right)\left(\ell+\frac{5}{2}\right)-(1+\eta)\left(\ell+\frac{3}{2}\right)+\eta\left(\frac{\ell}{2}+\frac{1}{4}\right)=1. \tag{B26}$$

Then we get $\alpha_{2\mathsf{k}} = \frac{C_1}{\mathsf{k}} + O(\frac{1}{\mathsf{k}^2})$, which leads to the divergence shown in Eq. (B11). To avoid the divergence, in the asymptotic behavior of $\alpha_{2\mathsf{k}}$ shown in Eq. (B24), only the second part should be nonzero. Taking $\alpha_{2\mathsf{k}} = \frac{C_2}{\mathsf{k}^{\zeta_2}}(\frac{\eta}{2+\eta})^{\mathsf{k}}$, we get

$$\left(1-\frac{\zeta_2}{\mathsf{k}}\right)\left(1+\frac{\eta}{2}\right)\left(1+\frac{2\ell+5}{2\mathsf{k}}\right)\eta^2-(1+\eta)\left(1+\frac{2\ell+3}{2\mathsf{k}}\right)\eta(2+\eta)+\left(1+\frac{\zeta_2}{\mathsf{k}}\right)\frac{\eta}{2}\left(1+\frac{2\ell+1}{2\mathsf{k}}\right)(2+\eta)^2+O\left(\frac{1}{\mathsf{k}^2}\right)=0, \tag{B27}$$

so the power ζ_2 is determined,

$$\zeta_2=\left[\left(1+\frac{\eta}{2}\right)\left(\ell+\frac{5}{2}\right)\eta^2-(1+\eta)\left(\ell+\frac{3}{2}\right)\eta(2+\eta)+\eta\left(\frac{\ell}{2}+\frac{1}{4}\right)(2+\eta)^2\right]\left[-\left(1+\frac{\eta}{2}\right)\eta^2+\frac{\eta}{2}(2+\eta)^2\right]^{-1}=1. \tag{B28}$$

Then we get the asymptotic behavior of $\alpha_{2\mathsf{k}}$,

$$\alpha_{2\mathsf{k}}=\left[\frac{C_2}{\mathsf{k}}+O\left(\frac{1}{\mathsf{k}^2}\right)\right]\left(\frac{\eta}{2+\eta}\right)^{\mathsf{k}}. \tag{B29}$$

To make $C_1 = 0$, κ should take discrete values. However, because $C_1 = 0$ is an asymptomatic condition for the sequence $\alpha_{2\mathsf{k}}$, we can only solve κ numerically. From the recursion relation for $\mathsf{k} \geqslant 0$,

$$\left[\frac{1}{2}\left(1+\frac{\eta}{2}\right)(\ell+2\mathsf{k}+2)(\ell+2\mathsf{k}+1)+\left(1+\frac{\eta}{2}\right)(\ell+2\mathsf{k}+2)-\frac{1}{2}\left(1+\frac{\eta}{2}\right)\ell(\ell+1)\right]\alpha_{2\mathsf{k}+2}$$
$$=\left[\frac{1}{2}(1+\eta)(\ell+2\mathsf{k})(\ell+2\mathsf{k}-1)+2(1+\eta)(\ell+2\mathsf{k})-\kappa-\frac{1}{2}(1+\eta)\ell(\ell+1)\right]\alpha_{2\mathsf{k}}$$
$$-\left[\frac{\eta}{4}(\ell+2\mathsf{k}-2)(\ell+2\mathsf{k}-3)+\frac{3}{2}\eta(\ell+2\mathsf{k}-2)-\frac{\eta}{4}\ell(\ell+1)\right]\alpha_{2\mathsf{k}-2}, \tag{B30}$$

where $\alpha_{-2} \equiv 0$, when α_0 is normalized to be 1, we can get $\alpha_{2\mathsf{k}_0+2}(\kappa)$ and $\alpha_{2\mathsf{k}_0}(\kappa)$ for some large enough integer k_0. Then, κ can be solved by [Eq. (42)]

$$\alpha_{2\mathsf{k}_0+2}=\alpha_{2\mathsf{k}_0}\frac{\mathsf{k}_0}{\mathsf{k}_0+1}\frac{\eta}{2+\eta}. \tag{B31}$$

Equation (B31) is an equation of order $(\mathsf{k}_0 + 1)$, so we will get $(\mathsf{k}_0 + 1)$ solutions of κ. When $k_0 \to \infty$, we should get infinite solutions of κ, which form a discrete spectrum. Note that when $\eta = 0$, Eq. (B31) becomes the condition that N in Eq. (B12) is finite, which is consistent with our previous result.

b. 2D case

Consider Eq. (40) with $\eta \neq 0$,

$$\frac{1}{2}\left[\left(1+\frac{\eta}{2}\right)-(1+\eta)r^2+\frac{\eta}{2}r^4\right]\frac{d^2\rho}{dr^2}+\frac{1}{2}\left[\left(1+\frac{\eta}{2}\right)-3(1+\eta)r^2+\frac{5\eta}{2}r^4\right]\frac{1}{r}\frac{d\rho}{dr}+\left\{\kappa r^2-\frac{1}{2}\mathsf{m}^2\left[\left(1+\frac{\eta}{2}\right)-(1+\eta)r^2+\frac{\eta}{2}r^4\right]\right\}\frac{\rho}{r^2}=0. \tag{B32}$$

We still have Eq. (B14). Taking $\mathsf{m} \geqslant 0$ for simplicity, we get a recursion relation,

$$\left[\frac{1}{2}\left(1+\frac{\eta}{2}\right)(\mathsf{m}+2\mathsf{k}+2)(\mathsf{m}+2\mathsf{k}+1)+\frac{1}{2}\left(1+\frac{\eta}{2}\right)(\mathsf{m}+2\mathsf{k}+2)-\frac{1}{2}\left(1+\frac{\eta}{2}\right)\mathsf{m}^2\right]\alpha_{2\mathsf{k}+2}$$
$$+\left[-\frac{1}{2}(1+\eta)(\mathsf{m}+2\mathsf{k})(\mathsf{m}+2\mathsf{k}-1)-\frac{3}{2}(1+\eta)(\mathsf{m}+2\mathsf{k})+\kappa+\frac{1}{2}(1+\eta)\mathsf{m}^2\right]\alpha_{2\mathsf{k}}$$
$$+\left[\frac{\eta}{4}(\mathsf{m}+2\mathsf{k}-2)(\mathsf{m}+2\mathsf{k}-3)+\frac{5}{4}\eta(\mathsf{m}+2\mathsf{k}-2)-\frac{\eta}{4}\mathsf{m}^2\right]\alpha_{2\mathsf{k}-2}=0. \tag{B33}$$

Then, $\mathsf{N} = \infty$, unless $\mathsf{m} = 0$ and $\mathsf{N} = 0$, because

$$\tfrac{1}{4}(\mathsf{m}+2\mathsf{N})(\mathsf{m}+2\mathsf{N}-1)+\tfrac{5}{4}(\mathsf{m}+2\mathsf{N})-\tfrac{1}{4}\mathsf{m}^2=\mathsf{m}(2\mathsf{N}+1)+\mathsf{N}(\mathsf{N}+2)\geqslant 0. \tag{B34}$$

When $\mathsf{N} = \infty$ and $\mathsf{k} \to \infty$, taking an expansion of k^{-1}, at the leading order we get the same results as Eqs. (B23) and

(B24). Taking $\alpha_{2\mathsf{k}} = \frac{C_1}{\mathsf{k}^{\zeta_1}}$, we get

$$\left(1-\frac{\zeta_1}{\mathsf{k}}\right)\left(1+\frac{\eta}{2}\right)\left(1+\frac{\mathsf{m}+2}{\mathsf{k}}\right)-(1+\eta)\left(1+\frac{\mathsf{m}+1}{\mathsf{k}}\right)+\left(1+\frac{\zeta_1}{\mathsf{k}}\right)\frac{\eta}{2}\left(1+\frac{\mathsf{m}}{\mathsf{k}}\right)+O\left(\frac{1}{\mathsf{k}^2}\right)=0; \tag{B35}$$

then,

$$\zeta_1=\left(1+\frac{\eta}{2}\right)(\mathsf{m}+2)-(1+\eta)(\mathsf{m}+1)+\eta\frac{\mathsf{m}}{2}=1, \tag{B36}$$

and we should take $C_1 = 0$ to make an eigenfunction convergent when $r \to 1$. Taking $\alpha_{2\mathsf{k}} = \frac{C_2}{\mathsf{k}^{\zeta_2}}(\frac{\eta}{2+\eta})^{\mathsf{k}}$, we get

$$\left(1-\frac{\zeta_2}{\mathsf{k}}\right)\left(1+\frac{\eta}{2}\right)\left(1+\frac{\mathsf{m}+2}{\mathsf{k}}\right)\eta^2-(1+\eta)\left(1+\frac{\mathsf{m}+1}{\mathsf{k}}\right)\eta(2+\eta)+\left(1+\frac{\zeta_2}{\mathsf{k}}\right)\frac{\eta}{2}\left(1+\frac{\mathsf{m}}{\mathsf{k}}\right)(2+\eta)^2+O\left(\frac{1}{\mathsf{k}^2}\right)=0, \tag{B37}$$

so

$$\zeta_2=-\left[\left(1+\frac{\eta}{2}\right)(\mathsf{m}+2)\eta^2-(1+\eta)(\mathsf{m}+1)\eta(2+\eta)+\frac{\eta}{2}\mathsf{m}(2+\eta)^2\right][\eta^2+2\eta]^{-1}=1, \tag{B38}$$

and Eq. (B31) is still valid to determine eigenvalues numerically.

3. Orthonormal relation

The linear differential operators in Eqs. (B19) and (B32) are non-Hermitian if we use the simplest definition of an inner product in a Hilbert space, so we need to apply the Sturm-Liouville theory [81] to find proper definitions of the inner product. For an eigenfunction of a second-order linear differential operator,

$$P(r)\frac{d^2\rho}{dr^2}+Q(r)\frac{d\rho}{dr}+[\kappa W(r)-S(r)]\rho=0, \tag{B39}$$

it has a Sturm-Liouville form,

$$\frac{d}{dr}\left[p(r)\frac{d\rho}{dr}\right]+[\kappa w(r)-s(r)]\rho=0, \tag{B40}$$

where

$$p(r)=e^{\int\frac{Q(r)}{P(r)}dr},\quad w(r)=\frac{W(r)}{P(r)}e^{\int\frac{Q(r)}{P(r)}dr},$$
$$s(r)=\frac{S(r)}{P(r)}e^{\int\frac{Q(r)}{P(r)}dr}. \tag{B41}$$

Taking the 3D case as an example, when a boundary condition is satisfied,

$$p(r)\left[\rho_{\mathsf{n}_2,\ell}\frac{d\rho^*_{\mathsf{n}_1,\ell}}{dr}-\rho^*_{\mathsf{n}_1,\ell}\frac{d\rho_{\mathsf{n}_2,\ell}}{dr}\right]\Bigg|_{r=0}^{r=1}=0, \tag{B42}$$

the eigenfunctions can be normalized to form an orthonormal basis with an inner product,

$$(\rho_{\mathsf{n}_1,\ell},\rho_{\mathsf{n}_2,\ell})\equiv\int_0^1\frac{w(r)}{w}\rho^*_{\mathsf{n}_1,\ell}(r)\rho_{\mathsf{n}_2,\ell}(r)dr=\delta_{\mathsf{n}_1,\mathsf{n}_2}, \tag{B43}$$

where w is an arbitrary coefficient.

a. 3D case

In the 3D case,

$$p(r)=e^{\int\frac{Q(r)}{P(r)}dr}=\exp\left\{\int\frac{\left(1+\frac{\eta}{2}\right)-2(1+\eta)r^2+\frac{3}{2}\eta r^4}{\frac{r}{2}\left[\left(1+\frac{\eta}{2}\right)-(1+\eta)r^2+\frac{\eta}{2}r^4\right]}dr\right\}=r^2(1-r^2)(2+\eta-\eta r^2), \tag{B44}$$

$$w(r)=\frac{2}{\left(1+\frac{\eta}{2}\right)-(1+\eta)r^2+\frac{\eta}{2}r^4}r^2(1-r^2)(2+\eta-\eta r^2)=4r^2, \tag{B45}$$

$$s(r)=\ell(\ell+1)(1-r^2)(2+\eta-\eta r^2). \tag{B46}$$

Near $r = 0$, we have $\rho(r) \sim r^\ell$. Near $r = 1$, we have required that $\rho(r)$ is finite, and by an expansion of $1 - r$, we have $\frac{d\rho}{dr} = \kappa\rho$, so $\frac{d\rho}{dr}$ is also finite. Because $p(0) = p(1) = 0$, for two different eigenfunctions $\rho_{\mathsf{n}_1,\ell}(r)$ and $\rho_{\mathsf{n}_2,\ell}(r)$, the condition given by Eq. (B42) is satisfied. So we get the orthonormal relation in Eq. (43),

$$(\rho_{\mathsf{n}_1,\ell},\rho_{\mathsf{n}_2,\ell})\equiv\int_0^1 r^2\rho^*_{\mathsf{n}_1,\ell}(r)\rho_{\mathsf{n}_2,\ell}(r)dr=\delta_{\mathsf{n}_1,\mathsf{n}_2}, \tag{B47}$$

where we have taken $w = 4$ in Eq. (B43).

b. 2D case

In the 2D case,

$$p(r)=\exp\left\{\int\frac{\left(1+\frac{\eta}{2}\right)-3(1+\eta)r^2+\frac{5}{2}\eta r^4}{r\left[\left(1+\frac{\eta}{2}\right)-(1+\eta)r^2+\frac{\eta}{2}r^4\right]}dr\right\}=r(1-r^2)(2+\eta-\eta r^2), \tag{B48}$$

$$w(r)=4r,\quad s(r)=\frac{m^2}{r}(1-r^2)(2+\eta-\eta r^2). \tag{B49}$$

Taking $w = 4$, we get the orthonormal relation in Eq. (43),

$$(\rho_{\mathsf{n}_1,\mathsf{m}},\rho_{\mathsf{n}_2,\mathsf{m}})\equiv\int_0^1 r\rho^*_{\mathsf{n}_1,\mathsf{m}}(r)\rho_{\mathsf{n}_2,\mathsf{m}}(r)dr=\delta_{\mathsf{n}_1,\mathsf{n}_2}. \tag{B50}$$

APPENDIX C: DISCUSSIONS ON TIGHT-BINDING MODELS

In this Appendix, as a supplement to the continuous model given by Eqs. (1)–(3), we discuss Bloch wave-function effects in tight-binding models defined in discretized lattices. We first clarify a general tight-binding limit of the continuous model in Sec. C 1. We then focus on the simplest example, i.e., bipartite tight-binding models, and calculate their Bloch wave-function quantities in Sec. C 2.

1. General tight-binding limit

In the tight-binding limit, the integral of $\boldsymbol{r}$ in a unit cell is substituted by a summation of sublattice indices times the volume of a unit cell. Namely, our Hamiltonian becomes

$$\begin{aligned} H_0 =& \Omega_{\text{cell}}^2 \sum_{\boldsymbol{R},\boldsymbol{R}'} \sum_{\sigma,\sigma'=0}^{\mathsf{n}_s-1} a^\dagger_{\boldsymbol{R}+\boldsymbol{t}_\sigma,\sigma} (\boldsymbol{H}_{0,\text{eff}})_{\sigma,\sigma'} \\ &\times (\boldsymbol{R}-\boldsymbol{R}'+\boldsymbol{t}_\sigma-\boldsymbol{t}_{\sigma'}) a_{\boldsymbol{R}'+\boldsymbol{t}_{\sigma'},\sigma'} \\ &+ \frac{g_{\text{eff}}}{2}\Omega_{\text{cell}} \sum_{\boldsymbol{R}} \sum_{\sigma=0}^{\mathsf{n}_s-1} a^\dagger_{\boldsymbol{R}+\boldsymbol{t}_\sigma,\sigma} a^\dagger_{\boldsymbol{R}+\boldsymbol{t}_\sigma,\sigma} a_{\boldsymbol{R}+\boldsymbol{t}_\sigma,\sigma} a_{\boldsymbol{R}+\boldsymbol{t}_\sigma,\sigma} \\ &+ \Omega_{\text{cell}} \sum_{\boldsymbol{R}} \sum_{\sigma=0}^{\mathsf{n}_s-1} U(\boldsymbol{R}+\boldsymbol{t}_\sigma) a^\dagger_{\boldsymbol{R}+\boldsymbol{t}_\sigma,\sigma} a_{\boldsymbol{R}+\boldsymbol{t}_\sigma,\sigma}, \end{aligned} \tag{C1}$$

where σ and σ' are sublattice indices, $\boldsymbol{R}$ and $\boldsymbol{R}'$ take lattice vectors, n_s is the number of sublattices in a unit cell, and $\boldsymbol{t}_\sigma$ is the relative position of the σth sublattice in a unit cell. Different from a more commonly used convention that different sublattices in the same unit cell are regarded as in the same position, here we keep $\boldsymbol{t}_\sigma$ in Fourier transforms to make crystal symmetries more explicit. This convention results in discontinuity of a $\boldsymbol{k}$-space Hamiltonian at the boundary of the first Brillouin zone, but this is not a problem for us because we only care about the Bloch states near the band bottom.

In Eq. (C1), $U(\boldsymbol{R}+\boldsymbol{t}_\sigma) \equiv U(\boldsymbol{r}=\boldsymbol{R}+\boldsymbol{t}_\sigma)$ and its Fourier transform is defined in the continuous space as the general cases of the continuous model,

$$\begin{aligned} U(\boldsymbol{R}+\boldsymbol{t}_\sigma) &= \int_\infty \frac{d^d\boldsymbol{k}}{(2\pi)^d} e^{i\boldsymbol{k}\cdot(\boldsymbol{R}+\boldsymbol{t}_\sigma)} U_{\boldsymbol{k}} \\ &\approx \int_{\text{BZ}} \frac{d^d\boldsymbol{k}}{(2\pi)^d} e^{i\boldsymbol{k}\cdot(\boldsymbol{R}+\boldsymbol{t}_\sigma)} U_{\boldsymbol{k}}. \end{aligned} \tag{C2}$$

Because now $a_\sigma(\boldsymbol{R}+\boldsymbol{t}_\sigma)$ and $(H_{0,\text{eff}})_{\sigma,\sigma'}(\boldsymbol{R}-\boldsymbol{R}'+\boldsymbol{t}_\sigma-\boldsymbol{t}_{\sigma'})$ are defined in the lattice, to recover the general result of the low-energy effective action in the Bloch basis, their Fourier transforms are defined by

$$a_{\boldsymbol{R}+\boldsymbol{t}_\sigma,\sigma} = \sum_{\mathsf{n}=0}^{\mathsf{n}_s-1} \int_{\text{BZ}} \frac{d^d\boldsymbol{k}}{(2\pi)^{\frac{d}{2}}} e^{i\boldsymbol{k}\cdot(\boldsymbol{R}+\boldsymbol{t}_\sigma)} u_{\mathsf{n},\boldsymbol{k},\sigma} b_{\mathsf{n},\boldsymbol{k}}, \tag{C3}$$

$$\begin{aligned} &(\boldsymbol{H}_{0,\text{eff}})_{\sigma,\sigma'}(\boldsymbol{R}-\boldsymbol{R}'+\boldsymbol{t}_\sigma-\boldsymbol{t}_{\sigma'}) \\ &= \sum_{\mathsf{n},\mathsf{n}'=0}^{\mathsf{n}_s-1} \int_{\text{BZ}} \frac{d^d\boldsymbol{k}}{(2\pi)^d} e^{i\boldsymbol{k}\cdot(\boldsymbol{R}-\boldsymbol{R}'+\boldsymbol{t}_\sigma-\boldsymbol{t}_{\sigma'})} (\boldsymbol{H}_{0,\text{eff}})_{\sigma,\sigma',\boldsymbol{k}} \\ &= \sum_{\mathsf{n},\mathsf{n}'=0}^{\mathsf{n}_s-1} \int_{\text{BZ}} \frac{d^d\boldsymbol{k}}{(2\pi)^d} e^{i\boldsymbol{k}\cdot(\boldsymbol{R}-\boldsymbol{R}'+\boldsymbol{t}_\sigma-\boldsymbol{t}_{\sigma'})} u^*_{\mathsf{n},\boldsymbol{k},\sigma} u_{\mathsf{n},\boldsymbol{k},\sigma'} (\boldsymbol{H}_{0,\text{eff}})_{\mathsf{n},\boldsymbol{k}}, \end{aligned} \tag{C4}$$

where n is the band index, and $u_{\mathsf{n},\boldsymbol{k},\sigma}$ is the normalized eigenvector of $(\boldsymbol{H}_{0,\text{eff}})_{\sigma,\sigma',\boldsymbol{k}}$ in the sublattice space,

$$\sum_{\sigma=0}^{\mathsf{n}_s-1} u^*_{\mathsf{n},\boldsymbol{k},\sigma} u_{\mathsf{n}',\boldsymbol{k},\sigma} = \delta_{\mathsf{n},\mathsf{n}'}. \tag{C5}$$

Note that the interaction strength g_{eff} in Eq. (C1) is different from g in Eq. (3), so we add a subscript "eff" to emphasize this, although they play the same role for a low-energy effective theory. The tight-binding limit makes $M \to \infty$ and $g_{\text{eff}} = O(gM) \to \infty$. This is because atoms are constrained at only several points in the unit cell, which significantly enlarges the effective repulsive interaction. Though, as there must be finite widths of Wannier functions in reality, we can renormalize g_{eff} to be finite.

A Bloch wave-function quantity $M_{\mathsf{n},\text{eff}}$ is defined by

$$M_{\mathsf{n},\text{eff}}(\boldsymbol{k}) = \mathsf{n}_s \sum_{\sigma=0}^{\mathsf{n}_s-1} u^*_{\mathsf{n},\boldsymbol{k},\sigma} u^*_{\mathsf{n},\boldsymbol{k},\sigma} u_{\mathsf{n},\boldsymbol{k},\sigma} u_{\mathsf{n},\boldsymbol{k},\sigma}, \tag{C6}$$

and other Bloch wave-function quantities are defined similarly. When the sublattices become equivalent, $|u_{\mathsf{n},\boldsymbol{k},\sigma}| = \frac{1}{\sqrt{\mathsf{n}_s}}$ and $M_{\mathsf{n},\text{eff}}(\boldsymbol{k}) = 1$; for a general case, $|u_{\mathsf{n},\boldsymbol{k},\sigma}|$ depends on σ and $M_{\mathsf{n},\text{eff}}(\boldsymbol{k}) > 1$. We focus on the lowest band, i.e., $\mathsf{n} = 0$, whose dispersion is assumed to be $(\boldsymbol{H}_{0,\text{eff}})_{0,\boldsymbol{k}} = \frac{k^2}{2m} + O(k^3)$ near the band bottom $\boldsymbol{k} = \boldsymbol{0}$.

In the next section, we only consider the tight-binding limit and only discuss the quantities with the subscript "eff," so we will omit the subscript for convenience. We also omit the band index in $(\boldsymbol{H}_0)_{\boldsymbol{k}}$ when denoting a matrix and in $u_{\boldsymbol{k},\sigma}$ when denoting the lowest band.

2. Bloch wave-function quantities of bipartite tight-binding models

Next, we focus on bipartite lattices ($\mathsf{n}_s = 2$). For a 2D lattice, suppose there is a $\mathbb{Z}_n$ ($n \geqslant 3$) rotational symmetry; for a 3D lattice, suppose it belongs to the cubic crystal system. Near the band bottom $\boldsymbol{k} = \boldsymbol{0}$, in the sublattice space we can expand the single-body Hamiltonian by Pauli matrices,

$$\begin{aligned} (\boldsymbol{H}_0)_{\boldsymbol{k}} =& \tilde{h}_{\boldsymbol{k}} \sin\Theta_{\boldsymbol{k}} \cos\Phi_{\boldsymbol{k}} \boldsymbol{\sigma}_x + \tilde{h}_{\boldsymbol{k}} \sin\Theta_{\boldsymbol{k}} \sin\Phi_{\boldsymbol{k}} \boldsymbol{\sigma}_y \\ &+ \tilde{h}_{\boldsymbol{k}} \cos\Theta_{\boldsymbol{k}} \boldsymbol{\sigma}_z + \bar{h}_{\boldsymbol{k}} \boldsymbol{\sigma}_0, \end{aligned} \tag{C7}$$

where we neglect a constant which shifts the energy of $\boldsymbol{k} = \boldsymbol{0}$ of the lower band to be zero. Then the lower-band eigenvector is given by

$$\boldsymbol{u}_{\boldsymbol{k}} \equiv \begin{pmatrix} u_{\boldsymbol{k},1} \\ u_{\boldsymbol{k},2} \end{pmatrix} = \begin{pmatrix} -\sin\frac{\Theta_{\boldsymbol{k}}}{2} \\ \cos\frac{\Theta_{\boldsymbol{k}}}{2} e^{i\Phi_{\boldsymbol{k}}} \end{pmatrix}. \tag{C8}$$

The Hamiltonian near $\boldsymbol{k} = \boldsymbol{0}$ is constrained by the lattice symmetry,

$$\begin{aligned} (\boldsymbol{H}_0)_{\boldsymbol{k}} =& \left(a_x - \tfrac{1}{2}b_x k^2\right)\boldsymbol{\sigma}_x + \left(a_y - \tfrac{1}{2}b_y k^2\right)\boldsymbol{\sigma}_y \\ &+ \left(a_z - \tfrac{1}{2}b_z k^2\right)\boldsymbol{\sigma}_z + \tfrac{1}{2}b_0 k^2 \boldsymbol{\sigma}_0 + O(k^3). \end{aligned} \tag{C9}$$

For simplicity, we take $a_{x,y,z} \geqslant 0$, $b_{x,y,z,0} \geqslant 0$, and it can be generalized to other cases.

If there is a time-reversal symmetry, i.e., $(\boldsymbol{H}_0)^*_{\boldsymbol{k}} = (\boldsymbol{H}_0)_{-\boldsymbol{k}}$, then $a_y = b_y = 0$. If there is an inversion symmetry that exchanges two sublattices (e.g., 2D honeycomb lattice), i.e., $\boldsymbol{\sigma}_x(\boldsymbol{H}_0)_{\boldsymbol{k}}\boldsymbol{\sigma}_x = (\boldsymbol{H}_0)_{-\boldsymbol{k}}$, then $a_y = b_y = a_z = b_z = 0$. If there is an inversion symmetry that keeps the sublattices invariant (e.g., 2D bipartite square lattice), i.e., $(\boldsymbol{H}_0)_{\boldsymbol{k}} = (\boldsymbol{H}_0)_{-\boldsymbol{k}}$, it does not give additional constraints to Eq. (C9). In addition, we take the permutation of sublattices as our definition of the sublattice symmetry, i.e., $\boldsymbol{\sigma}_x(\boldsymbol{H}_0)_{\boldsymbol{k}}\boldsymbol{\sigma}_x = (\boldsymbol{H}_0)_{\boldsymbol{k}}$, which is

different from a conventional one, i.e., $\boldsymbol{\sigma}_z(\boldsymbol{H}_0)_{\boldsymbol{k}}\boldsymbol{\sigma}_z = -(\boldsymbol{H}_0)_{\boldsymbol{k}}$. The sublattice symmetry requires $a_y = b_y = a_z = b_z = 0$.

We can calculate the Bloch wave-function quantities near $\boldsymbol{k} = \boldsymbol{0}$, which are much simplified by $\partial_{k_x}\Theta_{\boldsymbol{0}} = \partial_{k_x}\Phi_{\boldsymbol{0}} = 0$,

$$M_d(\boldsymbol{k}) = M(\boldsymbol{k}) - 1 = 2\left(\sin^4\frac{\Theta_{\boldsymbol{k}}}{2} + \cos^4\frac{\Theta_{\boldsymbol{k}}}{2}\right) - 1 = \cos^2\Theta_{\boldsymbol{k}}, \tag{C10}$$

$$\partial_{k_x}M(\boldsymbol{k}) = -\sin 2\Theta_{\boldsymbol{k}}\partial_{k_x}\Theta_{\boldsymbol{k}}, \tag{C11}$$

$$M''(\boldsymbol{0}) = \partial_{k_x}^2 M(\boldsymbol{0}) = -\sin 2\Theta_{\boldsymbol{0}}\partial_{k_x}^2\Theta_{\boldsymbol{0}}, \tag{C12}$$

$$\partial_{k_x}\boldsymbol{u}_{\boldsymbol{k}} = \begin{pmatrix} -\frac{1}{2}\left(\partial_{k_x}\Theta_{\boldsymbol{k}}\right)\cos\frac{\Theta_{\boldsymbol{k}}}{2} \\ -\frac{1}{2}\left(\partial_{k_x}\Theta_{\boldsymbol{k}}\right)\sin\frac{\Theta_{\boldsymbol{k}}}{2}e^{i\Phi_{\boldsymbol{k}}} + i\left(\partial_{k_x}\Phi_{\boldsymbol{k}}\right)\cos\frac{\Theta_{\boldsymbol{k}}}{2}e^{i\Phi_{\boldsymbol{k}}} \end{pmatrix}, \tag{C13}$$

$$\partial_{k_x}^2\boldsymbol{u}_{\boldsymbol{0}} = \begin{pmatrix} -\frac{1}{2}\left(\partial_{k_x}^2\Theta_{\boldsymbol{0}}\right)\cos\frac{\Theta_{\boldsymbol{0}}}{2} \\ -\frac{1}{2}\left(\partial_{k_x}^2\Theta_{\boldsymbol{0}}\right)\sin\frac{\Theta_{\boldsymbol{0}}}{2}e^{i\Phi_{\boldsymbol{0}}} + i\left(\partial_{k_x}^2\Phi_{\boldsymbol{0}}\right)\cos\frac{\Theta_{\boldsymbol{0}}}{2}e^{i\Phi_{\boldsymbol{0}}} \end{pmatrix}, \tag{C14}$$

$$\begin{aligned} S(\boldsymbol{0}) &= \mathrm{Im}\left[2\sum_{\sigma=0}^{1} u_{\boldsymbol{0},\sigma}^* u_{\boldsymbol{0},\sigma}^* u_{\boldsymbol{0},\sigma}\partial_{k_x^2}u_{\boldsymbol{0},\sigma} - M(\boldsymbol{0})\sum_{\sigma=0}^{1} u_{\boldsymbol{0},\sigma}^*\partial_{k_x^2}u_{\boldsymbol{0},\sigma}\right] \\ &= 2\cos^4\frac{\Theta_{\boldsymbol{0}}}{2}\partial_{k_x}^2\Phi_{\boldsymbol{0}} - (1+\cos^2\Theta_{\boldsymbol{0}})\cos^2\frac{\Theta_{\boldsymbol{0}}}{2}\partial_{k_x}^2\Phi_{\boldsymbol{0}} \\ &= \frac{1}{4}\sin 2\Theta_{\boldsymbol{0}}\partial_{k_x}^2\Phi_{\boldsymbol{0}}. \end{aligned} \tag{C15}$$

When there is the time-reversal symmetry, we get $\Phi_{\boldsymbol{k}} = 0$, so $S(\boldsymbol{k}) = 0$. When there is the sublattice symmetry or a 3D inversion symmetry that exchanges the two sublattices, we get $\cos\Theta_{\boldsymbol{0}} = 0$, so $M_d(\boldsymbol{0}) = M''(\boldsymbol{0}) = S(\boldsymbol{0}) = 0$, where there are no lattice-induced wave-function effects in the low-energy effective theory.

When the sublattice symmetry and the time-reversal symmetry are weakly broken, $\frac{a_y}{a_x}$, $\frac{b_y}{b_x}$, $\frac{a_z}{a_x}$, and $\frac{b_z}{b_x}$ are small. Then, at the leading order, we get

$$m \approx \frac{1}{b_0 + b_x}, \quad M_d(\boldsymbol{0}) \approx \frac{a_z^2}{a_x^2}, \tag{C16}$$

$$\Theta_{\boldsymbol{k}} = \frac{\pi}{2} - \arctan\frac{a_z - \frac{1}{2}b_z k^2}{\sqrt{\left(a_x - \frac{1}{2}b_x k^2\right)^2 + \left(a_y - \frac{1}{2}b_y k^2\right)^2}},$$
$$\Phi_{\boldsymbol{k}} = \arctan\frac{a_y - \frac{1}{2}b_y k^2}{a_x - \frac{1}{2}b_x k^2}, \tag{C17}$$

$$\begin{aligned} \partial_{k_x}^2\Theta_{\boldsymbol{0}} &= 2\frac{\partial\Theta_{\boldsymbol{0}}}{\partial k^2} \\ &= \frac{1}{1+\frac{a_z^2}{a_x^2+a_y^2}}\left[\frac{b_z}{\left(a_x^2+a_y^2\right)^{\frac{1}{2}}} - \frac{1}{2}\frac{2a_z(a_xb_x+a_yb_y)}{\left(a_x^2+a_y^2\right)^{\frac{3}{2}}}\right] \\ &\approx \frac{b_z}{a_x} - \frac{b_xa_z}{a_x^2}, \end{aligned} \tag{C18}$$

$$\begin{aligned} \partial_{k_x}^2\Phi_{\boldsymbol{0}} &= 2\frac{\partial\Phi_{\boldsymbol{0}}}{\partial k^2} = -\frac{1}{1+\frac{a_y^2}{a_x^2}}\frac{a_xb_y - a_yb_x}{a_x^2} \\ &\approx -\frac{b_y}{a_x} + \frac{b_xa_y}{a_x^2}, \end{aligned} \tag{C19}$$

$$M''(\boldsymbol{0}) \approx -\frac{2a_z}{a_x}\left(\frac{b_z}{a_x} - \frac{b_xa_z}{a_x^2}\right),$$
$$S(\boldsymbol{0}) \approx -\frac{a_z}{2a_x}\left(\frac{b_y}{a_x} - \frac{b_xa_y}{a_x^2}\right). \tag{C20}$$

If $\frac{a_y}{a_x}$, $\frac{b_y}{b_x}$, $\frac{a_z}{a_x}$, and $\frac{b_z}{b_x}$ are in the same order, μ and a_x (or a bandwidth) are in the same order; then, without fine tuning, $M_d(\boldsymbol{0})$, $m\mu M''(\boldsymbol{0})$, and $m\mu S(\boldsymbol{0})$ are in the same order.

For the example given in Eq. (62), from Eq. (63) we get

$$b_0 = 2t_1a_0^2, \quad a_x = -t_2 - 4t_3\cos\theta_3,$$
$$b_x = -2t_3a_0^2\cos\theta_3, \tag{C21}$$

$$a_y = -4t_3\sin\theta_3, \quad b_y = -2t_3a_0^2\sin\theta_3,$$
$$a_z = \Delta, \quad b_z = 0. \tag{C22}$$

We can apply a gauge transformation to take an additional sign for $a_{x,y}$ and $b_{x,y}$ so that they become positive. The gauge transformation is in the sublattice space instead of the momentum space, which does not affect the Bloch wave-function quantities. When Δ and θ_3 are small, by taking Eqs. (C21) and (C22) into Eqs. (C16) and (C20), and keeping the leading order, we get the results of Eq. (64), where two terms in $S(\boldsymbol{0})$ have been combined,

$$\begin{aligned} S(\boldsymbol{0}) &= -\frac{\Delta}{2(t_2+4t_3)}\left[\frac{2t_3a_0^2\theta_3}{t_2+4t_3} - \frac{8t_3^2a_0^2\theta_3}{(t_2+4t_3)^2}\right] \\ &= -\frac{a_0^2t_2t_3\theta_3\Delta}{(t_2+4t_3)^3}. \end{aligned} \tag{C23}$$

[1] J. M. Luttinger and W. Kohn, Motion of electrons and holes in perturbed periodic fields, Phys. Rev. **97**, 869 (1955).

[2] C. Kittle, *Introduction to Solid State Physics* (Wiley, Hoboken, NJ, 2004).

[3] A. P. Schnyder, S. Ryu, A. Furusaki, and A. W. W. Ludwig, Classification of topological insulators and superconductors in three spatial dimensions, Phys. Rev. B **78**, 195125 (2008).

[4] A. P. Schnyder, S. Ryu, A. Furusaki, and A. W. W. Ludwig, Classification of topological insulators and superconductors, AIP Conf. Proc. **1134**, 10 (2009).

[5] A. Kitaev, Periodic table for topological insulators and superconductors, AIP Conf. Proc. **1134**, 22 (2009).

[6] S. Ryu, A. P. Schnyder, A. Furusaki, and A. W. W. Ludwig, Topological insulators and superconductors: Tenfold way and dimensional hierarchy, New J. Phys. **12**, 065010 (2010).

[7] Z. Gong, Y. Ashida, K. Kawabata, K. Takasan, S. Higashikawa, and M. Ueda, Topological phases of non-Hermitian systems, Phys. Rev. X **8**, 031079 (2018).

[8] K. Kawabata, K. Shiozaki, M. Ueda, and M. Sato, Symmetry and topology in non-Hermitian physics, Phys. Rev. X **9**, 041015 (2019).

[9] K. v. Klitzing, G. Dorda, and M. Pepper, New method for high-accuracy determination of the fine-structure constant based on quantized Hall resistance, Phys. Rev. Lett. **45**, 494 (1980).

[10] R. B. Laughlin, Quantized Hall conductivity in two dimensions, Phys. Rev. B **23**, 5632 (1981).

[11] D. J. Thouless, M. Kohmoto, M. P. Nightingale, and M. den Nijs, Quantized Hall conductance in a two-dimensional periodic potential, Phys. Rev. Lett. **49**, 405 (1982).

[12] F. D. M. Haldane, Model for a quantum Hall effect without Landau levels: Condensed-matter realization of the "Parity Anomaly," Phys. Rev. Lett. **61**, 2015 (1988).

[13] C.-Z. Chang, J. Zhang, X. Feng, J. Shen, Z. Zhang, M. Guo, K. Li, Y. Ou, P. Wei, L.-L. Wang, Z.-Q. Ji, Y. Feng, S. Ji, X. Chen, J. Jia, X. Dai, Z. Fang, S.-C. Zhang, K. He, Y. Wang *et al.*, Experimental observation of the quantum anomalous Hall effect in a magnetic topological insulator, Science **340**, 167 (2013).

[14] C. L. Kane and E. J. Mele, Quantum spin Hall effect in graphene, Phys. Rev. Lett. **95**, 226801 (2005).

[15] C. L. Kane and E. J. Mele, Z_2 Topological order and the quantum spin Hall effect, Phys. Rev. Lett. **95**, 146802 (2005).

[16] B. A. Bernevig and S.-C. Zhang, Quantum spin Hall effect, Phys. Rev. Lett. **96**, 106802 (2006).

[17] B. A. Bernevig, T. L. Hughes, and S.-C. Zhang, Quantum spin Hall effect and topological phase transition in HgTe quantum wells, Science **314**, 1757 (2006).

[18] M. König, S. Wiedmann, C. Brüne, A. Roth, H. Buhmann, L. W. Molenkamp, X.-L. Qi, and S.-C. Zhang, Quantum spin Hall insulator state in HgTe quantum wells, Science **318**, 766 (2007).

[19] S. Pancharatnam, Generalized theory of interference, and its applications, Proc. Indian Acad. Sci. **44**, 247 (1956).

[20] J. P. Provost and G. Vallee, Riemannian structure on manifolds of quantum states, Commun. Math. Phys. **76**, 289 (1980).

[21] M. V. Berry, Quantal phase factors accompanying adiabatic changes, Proc. R. Soc. London A **392**, 45 (1984).

[22] R. Karplus and J. M. Luttinger, Hall effect in ferromagnetics, Phys. Rev. **95**, 1154 (1954).

[23] M.-C. Chang and Q. Niu, Berry phase, hyperorbits, and the Hofstadter spectrum: Semiclassical dynamics in magnetic Bloch bands, Phys. Rev. B **53**, 7010 (1996).

[24] G. Sundaram and Q. Niu, Wave-packet dynamics in slowly perturbed crystals: Gradient corrections and Berry-phase effects, Phys. Rev. B **59**, 14915 (1999).

[25] N. Nagaosa, J. Sinova, S. Onoda, A. H. MacDonald, and N. P. Ong, Anomalous Hall effect, Rev. Mod. Phys. **82**, 1539 (2010).

[26] D. Xiao, M.-C. Chang, and Q. Niu, Berry phase effects on electronic properties, Rev. Mod. Phys. **82**, 1959 (2010).

[27] Y. Gao, S. A. Yang, and Q. Niu, Field induced positional shift of Bloch electrons and its dynamical implications, Phys. Rev. Lett. **112**, 166601 (2014).

[28] Z. Z. Du, C. M. Wang, H.-P. Sun, H.-Z. Lu, and X. C. Xie, Quantum theory of the nonlinear Hall effect, Nat. Commun. **12**, 5038 (2021).

[29] Z. Z. Du, H.-Z. Lu, and X. C. Xie, Nonlinear Hall effects, Nat. Rev. Phys. **3**, 744 (2021).

[30] C. Wang, Y. Gao, and D. Xiao, Intrinsic nonlinear Hall effect in antiferromagnetic tetragonal CuMnAs, Phys. Rev. Lett. **127**, 277201 (2021).

[31] J. Wang, H. Zeng, W. Duan, and H. Huang, Intrinsic nonlinear Hall detection of the néel vector for two-dimensional antiferromagnetic spintronics, Phys. Rev. Lett. **131**, 056401 (2023).

[32] A. Gao, Y.-F. Liu, J.-X. Qiu, B. Ghosh, T. V. Trevisan, Y. Onishi, C. Hu, T. Qian, H.-J. Tien, S.-W. Chen, M. Huang, D. Bérubé, H. Li, C. Tzschaschel, T. Dinh, Z. Sun, S.-C. Ho, S.-W. Lien, B. Singh, K. Watanabe *et al.*, Quantum metric nonlinear Hall effect in a topological antiferromagnetic heterostructure, Science **381**, 181 (2023).

[33] S. A. Parameswaran, R. Roy, and S. L. Sondhi, Fractional Chern insulators and the W_∞ algebra, Phys. Rev. B **85**, 241308(R) (2012).

[34] R. Roy, Band geometry of fractional topological insulators, Phys. Rev. B **90**, 165139 (2014).

[35] T. S. Jackson, G. Möller, and R. Roy, Geometric stability of topological lattice phases, Nat. Commun. **6**, 8628 (2015).

[36] Y.-Z. You, Z. Chen, X.-Q. Sun, and H. Zhai, Superfluidity of bosons in kagome lattices with frustration, Phys. Rev. Lett. **109**, 265302 (2012).

[37] A. Julku, G. M. Bruun, and P. Törmä, Quantum geometry and flat band Bose-Einstein condensation, Phys. Rev. Lett. **127**, 170404 (2021).

[38] A. Julku, G. M. Bruun, and P. Törmä, Excitations of a Bose-Einstein condensate and the quantum geometry of a flat band, Phys. Rev. B **104**, 144507 (2021).

[39] S. Peotta, K.-E. Huhtinen, and P. Törmä, Quantum geometry in superfluidity and superconductivity, arXiv:2308.08248.

[40] S. Peotta and P. Törmä, Superfluidity in topologically nontrivial flat bands, Nat. Commun. **6**, 8944 (2015).

[41] A. Julku, S. Peotta, T. I. Vanhala, D.-H. Kim, and P. Törmä, Geometric origin of superfluidity in the lieb-lattice flat band, Phys. Rev. Lett. **117**, 045303 (2016).

[42] L. Liang, T. I. Vanhala, S. Peotta, T. Siro, A. Harju, and P. Törmä, Band geometry, Berry curvature, and superfluid weight, Phys. Rev. B **95**, 024515 (2017).

[43] M. Iskin, Geometric contribution to the Goldstone mode in spin-orbit coupled Fermi superfluids, Phys. B: Condens. Matter **592**, 412260 (2020).

[44] Z. Wang, G. Chaudhary, Q. Chen, and K. Levin, Quantum geometric contributions to the BKT transition: Beyond mean field theory, Phys. Rev. B **102**, 184504 (2020).

[45] P. Törmä, S. Peotta, and B. A. Bernevig, Superconductivity, superfluidity and quantum geometry in twisted multilayer systems, Nat. Rev. Phys. **4**, 528 (2022).

[46] T. Kitamura, A. Daido, and Y. Yanase, Quantum geometric effect on Fulde-Ferrell-Larkin-Ovchinnikov superconductivity, Phys. Rev. B **106**, 184507 (2022).

[47] M. Iskin, Extracting quantum-geometric effects from Ginzburg-Landau theory in a multiband Hubbard model, Phys. Rev. B **107**, 224505 (2023).

[48] S. A. Chen and K. T. Law, The Ginzburg-Landau theory of flat band superconductors with quantum metric, Phys. Rev. Lett. **132**, 026002 (2024).

[49] J.-X. Hu, S. A. Chen, and K. T. Law, Anomalous coherence length in superconductors with quantum metric, arXiv:2308.05686.

[50] H. Tian, X. Gao, Y. Zhang, S. Che, T. Xu, P. Cheung, K. Watanabe, T. Taniguchi, M. Randeria, F. Zhang, C. N. Lau, and M. W. Bockrath, Evidence for Dirac flat band superconductivity enabled by quantum geometry, Nature (London) **614**, 440 (2023).

[51] M. Krämer, L. Pitaevskii, and S. Stringari, Macroscopic dynamics of a trapped Bose-Einstein condensate in the presence of 1D and 2D optical lattices, Phys. Rev. Lett. **88**, 180404 (2002).

[52] F. S. Cataliotti, L. Fallani, F. Ferlaino, C. Fort, P. Maddaloni, and M. Inguscio, Dynamics of a trapped Bose-Einstein condensate in the presence of a one-dimensional optical lattice, J. Opt. B: Quantum Semiclassic. Opt. **5**, S17 (2003).

[53] O. Morsch and M. Oberthaler, Dynamics of Bose-Einstein condensates in optical lattices, Rev. Mod. Phys. **78**, 179 (2006).

[54] S. Konabe and T. Nikuni, Hydrodynamics of superfluid Bose gases in an optical lattice at finite temperatures, J. Low Temp. Phys. **148**, 453 (2007).

[55] Y. Hu, Z. Liang, and B. Hu, Collective excitations of a trapped Bose-Einstein condensate in the presence of weak disorder and a two-dimensional optical lattice, Phys. Rev. A **81**, 053621 (2010).

[56] H. M. Price and N. R. Cooper, Effects of Berry curvature on the collective modes of ultracold gases, Phys. Rev. Lett. **111**, 220407 (2013).

[57] X.-H. Li, T.-P. Choy, and T.-K. Ng, Bose-Einstein-condensed cold atoms in a lattice system with k-space Berry curvature, Phys. Rev. A **95**, 033628 (2017).

[58] A. L. Subaşı and M. Iskin, Quantum-geometric perspective on spin-orbit-coupled Bose superfluids, Phys. Rev. A **105**, 023301 (2022).

[59] I. Lukin, A. Sotnikov, and A. Kruchkov, Unconventional superfluidity and quantum geometry of topological bosons, arXiv:2307.08748.

[60] C.-K. Li, Q. Niu, and J. Feng, Geometric effects in the effective-mass theory and topological optical superlattices, Phys. Rev. A **98**, 041603(R) (2018).

[61] F. Evers and A. D. Mirlin, Anderson transitions, Rev. Mod. Phys. **80**, 1355 (2008).

[62] H. Zhai, *Ultracold Atomic Physics* (Cambridge University Press, Cambridge, 2021).

[63] L. Pitaevskii and S. Stringari, Elementary excitations in trapped Bose-Einstein condensed gases beyond the mean-field approximation, Phys. Rev. Lett. **81**, 4541 (1998).

[64] E. Braaten and J. Pearson, Semiclassical corrections to the oscillation frequencies of a trapped Bose-Einstein condensate, Phys. Rev. Lett. **82**, 255 (1999).

[65] S. Stringari, Collective excitations of a trapped Bose-condensed gas, Phys. Rev. Lett. **77**, 2360 (1996).

[66] V. M. Pérez-García, H. Michinel, J. I. Cirac, M. Lewenstein, and P. Zoller, Low energy excitations of a Bose-Einstein condensate: A time-dependent variational analysis, Phys. Rev. Lett. **77**, 5320 (1996).

[67] F. Dalfovo, S. Giorgini, L. P. Pitaevskii, and S. Stringari, Theory of Bose-Einstein condensation in trapped gases, Rev. Mod. Phys. **71**, 463 (1999).

[68] R. Onofrio, D. S. Durfee, C. Raman, M. Köhl, C. E. Kuklewicz, and W. Ketterle, Surface excitations of a Bose-Einstein condensate, Phys. Rev. Lett. **84**, 810 (2000).

[69] T.-L. Ho and V. B. Shenoy, Local spin-gauge symmetry of the Bose-Einstein condensates in atomic gases, Phys. Rev. Lett. **77**, 2595 (1996).

[70] Y.-J. Lin, R. L. Compton, K. Jiménez-García, J. V. Porto, and I. B. Spielman, Synthetic magnetic fields for ultracold neutral atoms, Nature (London) **462**, 628 (2009).

[71] W. Zheng and H. Zhai, Floquet topological states in shaking optical lattices, Phys. Rev. A **89**, 061603(R) (2014).

[72] I. Bloch, Ultracold quantum gases in optical lattices, Nat. Phys. **1**, 23 (2005).

[73] G.-B. Jo, J. Guzman, C. K. Thomas, P. Hosur, A. Vishwanath, and D. M. Stamper-Kurn, Ultracold atoms in a tunable optical kagome lattice, Phys. Rev. Lett. **108**, 045305 (2012).

[74] L. Tarruell, D. Greif, T. Uehlinger, G. Jotzu, and T. Esslinger, Creating, moving and merging Dirac points with a Fermi gas in a tunable honeycomb lattice, Nature (London) **483**, 302 (2012).

[75] G. Jotzu, M. Messer, R. Desbuquois, M. Lebrat, T. Uehlinger, D. Greif, and T. Esslinger, Experimental realization of the topological Haldane model with ultracold fermions, Nature (London) **515**, 237 (2014).

[76] S. Taie, H. Ozawa, T. Ichinose, T. Nishio, S. Nakajima, and Y. Takahashi, Coherent driving and freezing of bosonic matter wave in an optical Lieb lattice, Sci. Adv. **1**, e1500854 (2015).

[77] L. M. Aycock, H. M. Hurst, D. K. Efimkin, D. Genkina, H.-I. Lu, V. M. Galitski, and I. B. Spielman, Brownian motion of solitons in a Bose-Einstein condensate, Proc. Natl. Acad. Sci. **114**, 2503 (2017).

[78] H. R. Sadeghpour, J. L. Bohn, M. J. Cavagnero, B. D. Esry, I. I. Fabrikant, J. H. Macek, and A. R. P. Rau, Collisions near threshold in atomic and molecular physics, J. Phys. B: At., Mol. Opt. Phys. **33**, R93 (2000).

[79] C. Chin, R. Grimm, P. Julienne, and E. Tiesinga, Feshbach resonances in ultracold gases, Rev. Mod. Phys. **82**, 1225 (2010).

[80] When $-2 < \eta \leqslant -1$, the series diverges at $r = 1$. However, we cannot conclude that there is no solution to the differential equation. Further study is needed for whether the ground state is stable and whether there is a discrete dispersion of collective modes in this case.

[81] J. Mathews and R. L. Walker, *Mathematical Methods of Physics* (Addison-Wesley, Boston, 1971).

[82] An effect of W can be shown in a higher-order contribution to the density distribution of the ground state in the external potential.

[83] M. H. Anderson, J. R. Ensher, M. R. Matthews, C. E. Wieman, and E. A. Cornell, Observation of Bose-Einstein condensation in a dilute atomic vapor, Science **269**, 198 (1995).

[84] K. B. Davis, M. O. Mewes, M. R. Andrews, N. J. van Druten, D. S. Durfee, D. M. Kurn, and W. Ketterle, Bose-Einstein condensation in a gas of sodium atoms, Phys. Rev. Lett. **75**, 3969 (1995).

[85] B. Hetényi and P. Lévay, Fluctuations, uncertainty relations, and the geometry of quantum state manifolds, Phys. Rev. A **108**, 032218 (2023).

[86] G. Salerno, T. Ozawa, and P. Törmä, Drude weight and the many-body quantum metric in one-dimensional Bose systems, Phys. Rev. B **108**, L140503 (2023).

[87] P. Törmä, Essay: Where can quantum geometry lead us? Phys. Rev. Lett. **131**, 240001 (2023).